

QUANTUM REALIZATION OF THE FINITE ELEMENT METHOD

M. DEIML[†], D. PETERSEIM^{†*}

ABSTRACT. This paper presents a quantum algorithm for the solution of prototypical second-order linear elliptic partial differential equations discretized by d -linear finite elements on Cartesian grids of a bounded d -dimensional domain. An essential step in the construction is a BPX preconditioner, which transforms the linear system into a sufficiently well-conditioned one, making it amenable to quantum computation. We provide a constructive proof demonstrating that our quantum algorithm can compute suitable functionals of the solution to a given tolerance \mathbf{tol} with a complexity linear in \mathbf{tol}^{-1} for a fixed dimension d , neglecting logarithmic terms. This complexity is proportional to that of its one-dimensional counterpart and improves previous quantum algorithms by a factor of order \mathbf{tol}^{-2} . We also detail the design and implementation of a quantum circuit capable of executing our algorithm, and present simulator results that support the quantum feasibility of the finite element method in the near future, paving the way for quantum computing approaches to a wide range of PDE-related challenges.

Key words. quantum computer, finite element method, multilevel preconditioning, BPX, fast solver

AMS subject classifications. 68Q12, 65N30, 65N55, 65F08

1. INTRODUCTION

Quantum computers have the potential to provide exponential speedups over classical computing paradigms, a prospect that holds particular promise for the field of computational mathematics. Among the most compelling applications of this quantum advantage is the solution of partial differential equations (PDEs) [MP16, CPP⁺13, Ber14, BCOW17, CL20, HJZ23], especially in high dimension. The ability to solve PDEs more efficiently could improve numerical simulation in numerous fields, including engineering and physics.

A prime example within the vast landscape of PDEs is the steady-state diffusion equation

$$(1.1) \quad -\operatorname{div}(A\nabla u) = f,$$

posed in a bounded domain $D \subset \mathbb{R}^d$, $d \in \mathbb{N}$, accompanied by homogeneous Dirichlet conditions $u = 0$ at the boundary of the domain ∂D . This equation serves as a building block for understanding various processes, from heat conduction and material diffusion for $d \leq 3$ to high-dimensional problems in quantum chemistry where $d \gg 3$, underscoring the broad implications of advancing its solution methods.

The conventional approach to discretizing the steady-state diffusion equation (1.1) utilizes the Galerkin finite element method. In cases of axis-aligned domains, such as the unit cube $D = [0, 1]^d$, the method of choice often involves continuous piecewise d -linear (Q1) finite elements on a Cartesian grid composed of $N \times \dots \times N = N^d$ cells. Even

Date: March 29, 2024.

The work of D. Peterseim is part of a project that has received funding from the European Research Council (ERC) under the European Union's Horizon 2020 research and innovation programme (Grant agreement No. 865751 – RandomMultiScales).

under regularity assumptions on the symmetric and positive definite diffusion coefficient A and the right-hand side function f that ensure the $H^2(D)$ regularity of the solution $u = u_{A,f}$, the grid resolution N must scale inversely with the tolerance tol to reliably push the approximation error below this threshold. Consequently, achieving a desired tolerance $\text{tol} > 0$ requires a computational complexity that grows as tol^{-d} . This exponential growth of complexity with respect to the physical dimension d – a phenomenon often referred to as the curse of dimensionality – epitomizes the limitations of traditional PDE solution algorithms on classical computing systems, especially under conditions of moderate regularity [BG04].

Quantum computing offers promising ways to overcome the computational hurdles posed by high-dimensional PDEs. Among the notable strategies is *Schrödingerization*, which converts the original problem into a higher-dimensional Schrödinger equation solvable in theory with quantum efficiency [JLY23, HJZ23]. Another approach is to treat the linear systems derived from the PDE discretization with quantum linear system algorithms [HHL09, Amb10, BCK15, CKS17, GSW19, SSO19, LT20, AL22]. Similar methods are being explored in the context of variational quantum computing for finite element discretizations [TLDE23, SWR⁺23]. However, all methods face significant challenges, most importantly the poor conditioning associated with conventional finite difference or finite element discretizations, which deteriorates quadratically with increasing tolerance tol^{-1} under $H^2(D)$ regularity assumptions. It directly affects the efficiency of quantum linear system solvers, whose complexity grows linearly with the condition number and, thus, again quadratically with tol^{-1} . This represents a major obstacle to a direct quantum adaptation of standard computational PDE techniques. Furthermore, the practical implementation is currently limited by the depth of the resulting quantum circuits, which must scale at least linearly with the condition number, adding another layer of complexity to their realization.

The challenges highlighted above underscore the urgent need to overcome the limitations of current quantum computing approaches to solving PDEs. This leads us directly to the critical role of preconditioning in the quantum computing context. In classical computing, preconditioning is a well-established practice aimed at accelerating iterative solvers by improving the conditioning of the problem. In quantum computing, however, the importance of preconditioning extends beyond mere acceleration. It becomes essential for maintaining the scale of the amplitude of the solution state and preventing the amplification of input errors – a phenomenon similar to error amplification in classical computations with finite-precision arithmetic.

The straightforward application of conventional preconditioners, designed for classical systems to approximate the inverse system matrix efficiently, is not feasible. These operations could introduce ill-conditioned behavior, exacerbating the challenges in quantum computing. Previous attempts to repurpose preconditioning as a means to improve quantum computational runtimes [CJS13, BNWAG23, SX18] have generally met with limited success. A notable exception is the methodology introduced in [TAWL21], demonstrating an efficient resolution for the Laplace equation under very specific conditions – constant coefficients and periodic boundary conditions. However, this approach’s reliance on near diagonalization of the system of equations by a Fourier transform prevents its application to a wider range of PDEs beyond periodicity structures.

Given the challenges that ill-conditioning poses to quantum solvers, this work aims to demonstrate the feasibility of the finite element method on quantum computers and its

advantageous performance. Central to our approach is a re-evaluation of preconditioning strategies suitable for quantum environments, in which the classical BPX multilevel preconditioner [BPX90] from classical computers is adapted to the quantum context by integrating it with an appropriate stiffness matrix factorization to avoid ill-conditioned operations. This adaptation results in a practical algorithm with complexity $\mathcal{O}(\text{tol}^{-1})$, which is optimal with respect to tol^{-1} under reasonable assumptions. For fixed dimension d , this complexity is proportional to that of its one-dimensional counterpart as $\text{tol} \rightarrow 0$. The hidden constant in the \mathcal{O} notation may be affected by the dimension d , however. Notably, our algorithm not only achieves the efficiency of [TAWL21] for the periodic Laplacian, but also significantly improves the performance of the aforementioned algorithms by a factor of tol^{-2} .

In classical computational frameworks, achieving such optimized complexity often depends on strict regularity conditions, such as those applied in the use of higher-order finite elements [Sch98]. Conversely, the use of low-order finite elements, as discussed here, lends itself to efficient compression by sparse grids or low-rank tensor methods, which exploit the tensor product structure of the problem and its diffusion coefficient as well as the discretization. We refer to [BG04] and [Bac23] for corresponding comprehensive reviews. In fact, tensor methods are conceptually very closely related to quantum computing [Vid03]. Our algorithmic solution utilizes factorizations of the discretized problem that have previously found application in this area [BK20], thus bridging efficient strategies on classical computers and the emerging quantum computing paradigm.

Notation. We use the standard bra-ket notation to denote quantum states, which are normalized vectors in $\mathbb{C}^{(2^n)}$ for some $n \in \mathbb{N}$. For this, the one-qubit states $|0\rangle$ and $|1\rangle$ denote the vectors $(1, 0)^T$ and $(0, 1)^T$, respectively. Similarly, if $0 \leq x \leq 2^n - 1$ is an unsigned n -bit integer, then $|x\rangle$ denotes the state of an n -qubit register storing said integer. More precisely, if x has base 2 representation $x_n \dots x_1$ with $x_j \in \{0, 1\}$ for $1 \leq j \leq n$, then

$$|x\rangle = |x_1\rangle \otimes \dots \otimes |x_n\rangle = (\delta_{jx})_{j=0}^{2^n-1}.$$

Chained kets or bras like $|a\rangle|b\rangle$ indicate the semantic partitioning of a state into registers and refer to the tensor product $|a\rangle|b\rangle = |a\rangle \otimes |b\rangle$. Finally, for normalized vectors $v \in \mathbb{C}^{(2^n)}$ we sometimes write $|v\rangle$ instead of v . For any vector in “ket” notation, the corresponding “bra” means the conjugate transposed vector, i.e. $\langle \bullet | = |\bullet\rangle^\dagger$. An optional subscript such as in $|0\rangle_1$ refers to the number of qubits n in the qubit register.

Additionally we use the “big O” notation $\mathcal{O}(\bullet)$ for asymptotic comparison of algorithms. There the hidden constants are independent of the discretization constants, but may depend on the dimension d and the diffusion coefficient A .

2. MODEL PROBLEM

The model problem considered in this paper is a prototypical second-order linear partial differential equation (1.1) with a homogeneous Dirichlet boundary condition on a bounded Lipschitz domain D in d spatial dimensions. For the sake of simplicity we restrict ourselves to the particular choice of the d -dimensional unit cube $D := [0, 1]^d$. For the treatment of more general domains, see Remark 6.5.

The solution space of the problem is the Sobolev space $H_0^1(D)$ and the associated bilinear form reads

$$(2.1) \quad a(u, v) = \int_D A \nabla u \cdot \nabla v \, dx$$

for $u, v \in H_0^1(D)$. The matrix-valued diffusion coefficient A is a function of the spatial variable x with measurable entries and is assumed to be symmetric positive definite. For simplicity, we assume that there are positive constants α and β such that

$$(2.2) \quad \alpha |\eta|^2 \leq \eta \cdot A \eta \leq \beta |\eta|^2$$

holds for all $\eta \in \mathbb{R}^d$ and almost all $x \in D$, where $|\eta|$ is the Euclidean norm of η . The condition (2.2) guarantees that the bilinear form (2.1) is an inner product on $H_0^1(D)$. It induces the energy norm $\|\cdot\|$, which is equivalent to the canonical norm on that space. Under the condition (2.2), the variational boundary value problem

$$(2.3) \quad a(u, v) = f^*(v), \quad v \in H_0^1(D),$$

has, according to the Lax-Milgram theorem, for all bounded linear functionals f^* on $H_0^1(D)$ a unique solution $u \in H_0^1(D)$.

The standard way of approximating the model problem (2.3) in a wide range of applications is the Galerkin method, i.e. restricting the variational problem to some finite dimensional subspace of $H_0^1(D)$. The most popular choice is the finite element space of continuous piecewise polynomial functions with respect to some suitable subdivision of the domain D . For our choice $D = [0, 1]^d$, let \mathcal{G}_h be the Cartesian grid of D of width $h = 2^{-L}$ for some $L \in \mathbb{N}$, i.e. the subdivision of D into 2^{dL} mutually distinct cubes of width h . We then consider the $Q1$ finite element space $\mathcal{V}_h \subset H_0^1(D)$ of continuous piecewise d -linear functions on that grid vanishing on the boundary ∂D . The unique solution $u_h \in \mathcal{V}_h$ of the discrete variational problem

$$(2.4) \quad a(u_h, v_h) = f^*(v_h)_{L^2}, \quad v_h \in \mathcal{V}_h,$$

is the best approximation of $u \in H_0^1(D)$ in the energy norm

$$(2.5) \quad \|u - u_h\| = \min_{v_h \in \mathcal{V}_h} \|u - v_h\|.$$

If the problem data are sufficiently smooth in the sense that the diffusion coefficient A is weakly differentiable with $\nabla A \in L^\infty(D, \mathbb{R}^{d \times d})$ and $f \in L^2(D)$ then $u \in H^2(D)$ and standard interpolation error estimates yield

$$(2.6) \quad \|u - u_h\| \leq C_{A,f} h,$$

where $C_{A,f}$ only depends on $\alpha, \beta, \|\nabla A\|_{L^\infty(D, \mathbb{R}^{d \times d})}$ and $\|f\|_{L^2(D)}$. The characteristic linear rate of convergence with respect to h is optimal under the regularity assumption. To ensure an error below the tolerance $\text{tol} > 0$ thus requires the choice $h \approx \text{tol}$ in general which implies that the number of degrees of freedom, and hence the computational cost on a classical computer, grows at least as tol^{-d} . Only under additional regularity assumptions can this unfavorable growth with the dimension d be relaxed. Classical options include the use of higher order finite elements [Sch98]. Its regularity requirements and convergence properties are analyzed even for the case of highly oscillatory multiscale coefficients in [PS12]. This approach has also been explored for quantum computers [CLO21]. Alternatively, the above choice of low-order finite elements can be efficiently compressed by sparse grids or low-rank tensor methods based on the tensor product structure of the

discretization introduced above for the special case of tensor product diffusion coefficients, see [BG04] and [Bac23] for corresponding reviews.

A choice of basis functions $\Lambda_1, \dots, \Lambda_N$ of \mathcal{V}_h transforms the discrete variational problem (2.4) into a system of $N := \dim \mathcal{V}_h = (2^L - 1)^d$ linear equations

$$Sc = r$$

for the coefficients $c = (c_1, \dots, c_N)^T$ of $u_h = \sum_{j=1}^N c_j \Lambda_j$ in its basis representation. The system matrix $S := (a(\Lambda_j, \Lambda_k))_{j,k=1}^N$ is given by the a -inner products of the basis functions, and the right hand side vector $r := ((f, \Lambda_j)_{L^2})_{j=1}^N$ contains the evaluation of the functional f^* in the basis functions. For the particular choice of hat (or Lagrange) basis functions Λ_j associated with the inner vertices x_j of \mathcal{G}_h which are uniquely characterized by the Lagrange property $\Lambda_j(x_k) = \delta_{jk}$ with the Kronecker delta δ_{jk} , the coefficient vector c contains exactly the nodal values $c_j = u_h(x_j)$. Furthermore, the matrix S is sparse with at most 3^d non-zero entries per row and column. In practice, the exact evaluation of the integrals underlying the entries of S and r is not always possible and a suitable quadrature is required. This case of a so-called variational crime [BS08] is well understood in the numerical analysis literature and will not be discussed in this manuscript. In particular, we implicitly assume that the diffusion coefficient A is well approximated by a piecewise constant function on the grid \mathcal{G}_h without further mention.

3. ENCODING VECTORS AND MATRICES ON QUANTUM COMPUTERS

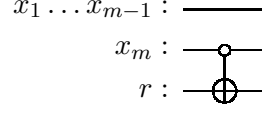
As a first step towards realizing a quantum implementation of the finite element method, we will address the necessary processing of vectors and matrices on a quantum computer. This so-called encoding is critical to realizing the potential speedup that quantum computing offers over traditional classical computing methods. For readers who are not familiar with the underlying basic principles of quantum computing, including qubits and quantum gates, we recommend the introductory article [Nan20]. For a more comprehensive mathematical overview we refer to [Lin22].

In quantum computing, a vector $c \in \mathbb{C}^{(2^m)}$ for $m \in \mathbb{N}$ is represented by a register of m qubits. Using the aforementioned Bra-ket notation, the canonical basis vectors $e_j \in \mathbb{C}^{(2^m)}$, where $(e_j)_k = \delta_{jk}$ for $j, k = 0, \dots, 2^m - 1$, are denoted as $|j\rangle$. In practice, this representation corresponds to a quantum state where the qubits in a register encode the integer j in binary, assigning one digit per qubit. The linear combination of basis vectors, $c_0 e_0 + \dots + c_{N-1} e_{2^m-1}$, is realized as a superposition $\sum_j c_j |j\rangle$ of basis states. It is imperative that these states are normalized to ensure admissibility on a quantum computer, which is satisfied when the Euclidean norm of c satisfies $|c| = 1$. Under this normalization condition, the resulting state is represented by $|c\rangle$.

To accommodate vectors whose norms are less than 1, we introduce an additional 1-qubit ancilla register. Such vectors can then be encoded as

$$\sum_j c_j |0\rangle |j\rangle + \sum_j \tilde{c}_j |1\rangle |j\rangle,$$

where \tilde{c}_j is chosen so that $\sum |\tilde{c}_j|^2 = 1 - |c|^2$. During a measurement of the state, the components of the original vector c can be detected by ignoring results where the ancilla bit is in the 1 state, effectively implementing a projective measurement that filters for the original vector space within an ambient superspace of dimension 2^{m+1} . Representing

FIGURE 3.1. The C_Π NOT gate for example 3.2

vectors with norms greater than 1 is not possible, and must be circumvented by appropriately rescaling the problem beforehand to ensure that all vectors fall within the admissible norm range.

In quantum computing, a matrix S is encoded not as a data structure stored in memory, but as an operation that transforms a basis state $|i\rangle$ into a superposition corresponding to the matrix-vector product of S and the basis vector represented by $|i\rangle$ (the i -th column of S if indexing starts at zero). This method relies on the inherently linear nature of quantum operations, ensuring that linear combinations of basis states are correctly mapped according to the action of the matrix. However, quantum transformations must also be unitary, i.e. norm preserving. Encoding arbitrary linear transformations thus requires embedding them in unitary transformations acting on higher dimensional spaces. Following the methodology outlined in [GSLW19], this is achieved by embedding S in the upper left block of a larger unitary matrix

$$(3.1) \quad U_S := \begin{bmatrix} \frac{1}{\gamma}S & \bullet \\ \bullet & \bullet \end{bmatrix},$$

where $\gamma > 0$ is a normalization constant that ensures that the spectral norm of $\frac{1}{\gamma}S$ remains bounded by 1, and \bullet denotes unspecified entries of the matrix necessary to make the full matrix unitary. In this formulation, $S = \gamma(\langle 0| \otimes \text{Id})U_S(|0\rangle \otimes \text{Id})$ is effectively represented by U_S , although the actual implementation of this encoding may vary. We will use U_S to refer to both the unitary matrix and its implementation interchangeably.

The operational effect of U_S on a quantum state can be succinctly described as

$$(\langle 0| \otimes \text{Id})U_S|0\rangle|i\rangle = \frac{1}{\gamma}S|i\rangle,$$

illustrating how a state $|0\rangle|i\rangle$ is mapped to another state that encodes the scaled action of S on $|i\rangle$. This process often requires more than one ancilla qubit for efficiency, leading to more general block encoding implementations as defined in [GSLW19]. Such implementations use projection operators to precisely embed the matrix S into the broader unitary operation U_S . The projections are conceptually linked to the previously discussed ancilla bit and encoded as generalized controlled NOT gates.

Definition 3.1 (Projection as C_Π NOT gate). Let $N, m \in \mathbb{N}$ with $N \leq 2^m$ and $\Pi : \mathbb{C}^{2^m} \rightarrow \mathbb{C}^N$ be a projection meaning a matrix with orthonormal rows. We call a gate of $m+1$ qubits a C_Π NOT gate if it flips the last bit if and only if the first m bits represent a vector in the range of Π , i.e. it performs the unitary operation

$$\Pi^\dagger \Pi \otimes (|0\rangle\langle 1| + |1\rangle\langle 0|) + (1 - \Pi^\dagger \Pi) \otimes \text{Id}.$$

Example 3.2 (C_{Π} NOT gate). Consider the projection $\Pi: \mathbb{C}^{(2^m)} \rightarrow \mathbb{C}^{(2^{m-1})}$ of a vector of length 2^m onto its first half

$$x \mapsto (x_0, \dots, x_{2^{m-1}-1})^T.$$

Then C_{Π} NOT can be implemented as a CNOT gate controlled by the m -th qubit being zero. See Figure 3.1 for the corresponding quantum circuit diagram.

The subsequent definition of block encodings of matrices uses such projection gates onto both the domain and the range of the matrices.

Definition 3.3 (Block encoding of a matrix, normalization and subnormalization). Let $N_1, N_2, m \in \mathbb{N}$ with $N_1, N_2 \leq M := 2^m$. Let $S \in \mathbb{C}^{N_2 \times N_1}$ and $\gamma \geq |S|$. Further let $\Pi_1: \mathbb{C}^M \rightarrow \mathbb{C}^{N_1}$ and $\Pi_2: \mathbb{C}^M \rightarrow \mathbb{C}^{N_2}$ be projections. Consider a quantum algorithm implementing a unitary matrix $U_S \in \mathbb{C}^{M \times M}$ and implementations of a C_{Π_1} NOT and a C_{Π_2} NOT gate. We call the triple $(U_S, C_{\Pi_1}\text{NOT}, C_{\Pi_2}\text{NOT})$ a *block-encoding* of S if

$$\gamma \Pi_2 U_S \Pi_1^\dagger = S.$$

The quantity $\gamma(U_S) := \gamma$ is called the *normalization factor* and $\tilde{\gamma}(U_S) := \gamma(U_S)/|S| \geq 1$ is called the *subnormalization factor*, where $|\bullet|$ denotes the spectral norm.

Remark 3.4. Definition 3.3 is related to the encoding of the matrix as a block of a unitary transformation as in (3.1). Specifically, the upper left $M \times M$ block \tilde{S} of the unitary

$$U_{\tilde{S}} := C_{\Pi_2}\text{NOT}(U_S \otimes \text{Id}) C_{\Pi_1}\text{NOT} \in \mathbb{C}^{2M \times 2M}$$

is equivalent to S up to an additional kernel and an additional cokernel that are orthogonal to $\mathbb{C}^{N_1}, \mathbb{C}^{N_2} \subset \mathbb{C}^M$. This can also be written as

$$\tilde{S} = \Pi_2^\dagger S \Pi_1.$$

The above definition of block encoding differs slightly from the one in [GSLW19, Lin22], where the number of ancilla bits and an approximation error of the encoding are used as additional parameters, while the subnormalization factor is not introduced. In the present context, the subnormalization is an important quantity that measures the extent to which the norm of a vector is preserved under the action of the block encoding, with $\tilde{\gamma}(U_S) = 1$ being optimal. We will see later that the computational complexity of solving a linear system is proportional to $\tilde{\gamma}(U_S) \cdot \kappa(S)$ and not just to $\kappa(S)$. The normalization factor $\gamma(U_S)$, on the other hand, tracks the relationship between the encoding and the actual matrix S . Knowing this quantity is essential to correctly interpret the result of applying the encoding to a vector.

Unitary matrices are trivially encoded by a circuit that implements them. In this case both Π_1 and Π_2 are identity matrices. However, trivial encoding is generally efficient only for “small” unitary matrices, i.e., those whose size does not depend on the problem size. To construct block encodings of larger and more complicated matrices, we will make use of the following algebra of block encodings. Therein, bounds for the normalization and subnormalization factors are quantified in terms of the condition number

$$\kappa(A) := |A| \cdot |A^+| = \sigma_{\max}(A)/\sigma_{\min}(A)$$

of a matrix A with maximal and minimal singular values $\sigma_{\max}(A)$ and $\sigma_{\min}(A)$. Here, \bullet^+ is the Moore-Penrose pseudoinverse so that $\kappa(A)$ is well defined even for rectangular matrices. Note that, $\kappa(A)$ may differ from the ratio of the largest and smallest eigenvalue $\lambda_{\max}(A)/\lambda_{\min}(A)$ in the case of square but non-symmetric matrices.

Proposition 3.5 (Operations on block encoded matrices). *Let $A \in \mathbb{C}^{m_A \times n_A}$, $B \in \mathbb{C}^{m_B \times n_B}$ with block encodings $(U_A, C_{\Pi_{A,1}} \text{NOT}, C_{\Pi_{A,2}} \text{NOT})$ and $(U_B, C_{\Pi_{B,1}} \text{NOT}, C_{\Pi_{B,2}} \text{NOT})$. Then block encodings with normalization γ and subnormalization $\tilde{\gamma}$ can be constructed for the following operations:*

$$(3.2a) \quad A \otimes B \quad \text{with } \gamma = \gamma(U_A)\gamma(U_B) \text{ and } \tilde{\gamma} = \tilde{\gamma}(U_A)\tilde{\gamma}(U_B),$$

$$(3.2b) \quad A^\dagger \quad \text{with } \gamma = \gamma(U_A) \text{ and } \tilde{\gamma} = \tilde{\gamma}(U_A)$$

$$(3.2c) \quad \begin{bmatrix} A & 0 \\ 0 & B \end{bmatrix} \quad \text{with } \gamma = \max\{\gamma(U_A), \gamma(U_B)\} \text{ and } \tilde{\gamma} = \max\{\tilde{\gamma}(U_A), \tilde{\gamma}(U_B)\},$$

$$(3.2d) \quad AB \quad \text{with } \gamma = \gamma(U_A)\gamma(U_B) \text{ and } \tilde{\gamma} \leq \begin{cases} \kappa(A)\tilde{\gamma}(U_A)\tilde{\gamma}(U_B) & \text{if } n_A \geq m_B, \\ \kappa(B)\tilde{\gamma}(U_A)\tilde{\gamma}(U_B) & \text{if } m_B \geq n_A, \end{cases}$$

$$(3.2e) \quad \begin{bmatrix} A & B \end{bmatrix} \quad \text{with } \gamma = \sqrt{\gamma(U_A)^2 + \gamma(U_B)^2} \text{ and } \tilde{\gamma} \leq \sqrt{\tilde{\gamma}(U_A)^2 + \tilde{\gamma}(U_B)^2},$$

$$(3.2f) \quad \mu_A A + \mu_B B \quad \text{for any } \mu_A, \mu_B \in \mathbb{C} \text{ with } \gamma = \sqrt{2(|\mu_1\gamma(U_A)| + |\mu_2\gamma(U_B)|)},$$

provided that the dimensions are compatible in the sense of $\Pi_{B,2} = \Pi_{A,1}$ in (3.2d), $\Pi_{A,2} = \Pi_{B,2}$ in (3.2e) and (3.2f), and $\Pi_{A,1} = \Pi_{B,1}$ in (3.2f). Without further assumptions, the subnormalization in (3.2f) can be unbounded.

The results for multiplication and linear combination are due to [GSLW19]. A complete proof of the proposition along with concrete quantum circuits is given in Appendix B. Note that in all cases, the subnormalization factor of the resulting block encoding can be calculated from Definition 3.3, as long as the spectral norm of the encoded matrix is known. This is especially useful for the addition of matrices, where an estimate of the spectral norm of the result requires further assumptions on the summands.

For the efficient treatment of the diffusion coefficient, we will later take advantage of the fact that block diagonal matrices can be efficiently implemented for many cases.

Proposition 3.6 (Block encoding of block diagonal matrices). *Let $n, m, N, M \in \mathbb{N}$ with $N = 2^n$ and $M \leq 2^m$. Let $\gamma > 0$ and $A \in NM \times NM$ be a $N \times N$ block diagonal matrix with blocks of size $M \times M$. Let $\Pi: \mathbb{C}^{(2^m)} \rightarrow \mathbb{C}^M$ be a projection with an implementation of $C_\Pi \text{NOT}$. Let U_A be a quantum circuit operating on two qubit registers $|j\rangle_n, |x\rangle_m$ applying a block encoding of the j -th diagonal block A_{jj} with the projection Π and normalization γ on the register $|x\rangle$, i.e.,*

$$\gamma(\langle j| \otimes \Pi)U_A(|j\rangle \otimes \Pi) = A_{jj}.$$

Then we can construct a block encoding of A with normalization γ . Its subnormalization is the minimum of the subnormalization over all blocks.

Proof. It is easy to see that U_A is a block encoding of A with the projection $\text{Id}_N \otimes \Pi$. To estimate of the subnormalization simply observe, that the spectral norm $|A|$ is the maximum of the spectral norms of all blocks. \square

Block encodings can also be efficiently implemented directly for other classes of matrices, such as sparse matrices or matrices that can be written as a linear combination of unitaries (LCU) [GSLW19]. However, it is clear that one cannot encode k bits of information without using $\mathcal{O}(k)$ operations, i.e. we cannot expect to encode arbitrary matrices of size N in less than $\mathcal{O}(N^2)$ operations. This applies analogously to vectors. Since we want to achieve runtimes faster than linear in N , this implies that the data must be compressed in

some way. In the finite element context, this means that we expect the diffusion coefficient entering the stiffness matrix S and the right-hand side $|r\rangle$ to be given by subroutines that compute specific integrals of either function. For details, see the Appendix A.

4. THE QUANTUM LINEAR SYSTEM PROBLEM

As outlined in Section 2 we want to use quantum computers to solve linear systems of the form

$$Sc = r$$

arising from a particular finite element discretization of the partial differential equation (1.1). Without loss of generality, it is assumed that $|S| = 1$ and $|r| = 1$. In practice, this assumption is easily removed by appropriate rescaling of the equation.

In the quantum context, we assume that the right-hand side is given as an oracle, i.e. an algorithm that we treat as a black box. The oracle should prepare the corresponding superposition $|r\rangle$, i.e. it maps the initial state $|0\rangle$ to the state $|r\rangle$. This is explained in detail in Appendix A. Further, we assume that the matrix S is given as a block encoding, although there are other input models, such as oracles that compute the sparsity structure and corresponding entries of the matrix. Since $|S^{-1}| = \kappa(S)$ it is not possible in general to find a state $|c\rangle$ such that

$$|r\rangle = (\langle 0| \otimes \text{Id}) U_S |0\rangle |c\rangle = S |c\rangle.$$

Such a $|c\rangle$ may exceed 1 in norm and thus may not be representable on a quantum computer. Instead, quantum solvers compute the normalized solution up to a tolerance as specified in the following definition.

Definition 4.1 (Quantum linear system algorithm). Let $\kappa > 0$, $\text{tol} > 0$. Consider an algorithm that takes as input two oracles, O_S , which applies a block encoding to a matrix S , and O_r , which prepares the state $|r\rangle$. We say that the algorithm solves the quantum linear system problem for condition $\kappa := \tilde{\gamma}(O_S)\kappa(S)$ and error tol , if it produces a state $|c\rangle$ such that

$$\left\| |c\rangle - \frac{S^{-1}|r\rangle}{|S^{-1}|r\rangle|} \right\| < \text{tol}.$$

The number of calls to each oracle in the algorithm is denoted by its *query complexity*. We also allow the algorithm to fail with a probability that is independent of κ and tol , in which case it should communicate the failure via an additional flag bit.

There are several algorithms for solving linear algebraic systems on quantum computers. The earliest algorithm [HHL09] constructs a state encoding $\frac{1}{\kappa} S |c\rangle$ and normalizes it by amplitude amplification, achieving a complexity of $\mathcal{O}(\kappa^2 \text{tol}^{-1})$. Recently it has been shown that it is possible to improve both the κ and tol dependence in the complexity bound, either by more complex techniques like variable-time amplitude amplification [Amb10, BCOW17], or by constructing the normalized state $|c\rangle$ directly, thus avoiding the amplification process [AL22, LT20]. For a detailed comparison of these near-optimal approaches, see [TAWL21, Appendix A]. Both algorithms achieve the favorable runtime quantified in the following theorem, and thus serve as a possible proof.

Theorem 4.2 (Existence of fast quantum linear system algorithms). *A solution of the quantum linear system problem in the sense of Definition 4.1 can be computed with query complexity of $\mathcal{O}(\kappa \text{poly} \log(\kappa \text{tol}^{-1}))$.*

Once the solution $|c\rangle$ is computed, the reliable measurement of all its components requires at least $\mathcal{O}(N/\text{tol})$ samples of the state $|c\rangle$ and thus $\mathcal{O}(N/\text{tol})$ runs of the solver algorithm, eliminating any advantage over classical computers. A quantum advantage can only be expected for computing partial information of $|c\rangle$. Typically, the goal is to measure some *quantity of interest* of $|c\rangle$, which is computed either as a product $\langle c|M|c\rangle$ with a unitary matrix M using the *Hadamard test* [AJL06] or as a linear functional

$$c \mapsto \langle m|c\rangle$$

represented by a vector $m \in \mathbb{C}^N$ using the *Swap Test* [BCWDW01]. This requires an efficient construction of the state $|m\rangle$, or the unitary transformation M . Note that even to measure a quantity of interest up to the tolerance tol , any solver algorithm must be run at least $\mathcal{O}(\text{tol}^{-1})$ times [Kit95, Md23], resulting in a total runtime of $\mathcal{O}(\kappa \text{tol}^{-1} \text{poly log}(\kappa \text{tol}^{-1}))$. This is not a phenomenon specific to linear systems. Estimating any quantity encoded as the phase of a quantum state, a process called *phase estimation*, requires at least $\mathcal{O}(\text{tol}^{-1})$ measurements [Md23], and thus it is reasonable to assume that computing any information about the solution to (1.1) using a quantum computer must be of complexity at least linear in tol^{-1} . In the context of the finite element method, this is consistent with the results of [MP16], where it is shown that the runtime of quantum algorithms solving (1.1) must scale at least polynomially in tol^{-1} . However, the optimal dependence on tol^{-1} is not achieved by trivially applying a quantum linear system algorithm to the linear system $Sc = r$. The condition number $\kappa(S) \in \mathcal{O}(h^{-2})$ introduces a multiplicative factor tol^{-2} , because $h \lesssim \text{tol}$ is required to ensure a sufficiently small discretization error according to (2.6). Instead, we use *preconditioning* to avoid the suboptimal scaling of the algorithms caused by the increasing condition number of the stiffness matrix for smaller tolerances.

5. QUANTUM PRECONDITIONING

Starting with a discussion of its challenges and limitations, this section focuses on preconditioning as an essential strategy for improving the performance of quantum computing methods. The concept of preconditioning, well known in classical computing for its effectiveness in improving the efficiency of iterative solvers, faces unique challenges and opportunities when applied to quantum computing. Given the fundamental differences of the quantum paradigm, in particular the requirement for unitary operations, traditional preconditioning techniques must be reevaluated and adapted. This adaptation is critical to address the conditioning issues that significantly impact the feasibility and efficiency of quantum algorithms for solving PDEs.

5.1. Challenges introduced by unitary transformation. Preconditioning is a technique that transforms a problem into a more favorable form for numerical solution, typically by left and right preconditioning of the form $P_1 S P_2 y = P_1 r$. We will focus on the case of *operator preconditioning* [Hip06], where P_1 and P_2 represent discretizations of linear operators, denoted as \mathcal{R}_1 and \mathcal{R}_2 . The classical application involves assembling the matrices P_1 , S , and P_2 , along with the vector r , to compute the right-hand side $P_1 r$. Iterative solvers then leverage this vector and the matrices for solving the preconditioned linear equation, ultimately leading to the solution of the original problem via $c = P_2 y$.

At first glance, one might imagine applying classical preconditioning strategies directly within the quantum framework. This would involve constructing a quantum state corresponding to the right-hand vector $|r\rangle$, finding block encodings for the matrices P_1 , S , and P_2 , and then computing the quantum equivalent of the matrix-vector product $|P_2 r\rangle$. With the matrix product $P_1 S P_2$ in hand, obtained through quantum-specific matrix-matrix multiplication (3.2d) from Proposition 3.5, one could then use a quantum linear system solver to generate a state $|y\rangle$. Ideally, this state $|y\rangle$, after further manipulation using the block encoding of P_2 , would yield the solution to the original problem. However, this approach runs into a fundamental limitation inherent to quantum computing: the spectral norm of any matrix implemented on a quantum computer must be bounded from above by 1. This limitation implies that multiplication by a matrix with a condition number κ could, in the worst case, decrease the norm of the resulting vector by a factor of κ . It is then impossible to reverse the loss of scale, a process called *amplitude amplification* [BH97, Gro98, Md23], without repeating all steps leading to the obtained state at least $\mathcal{O}(\kappa)$ times, to counteract the loss of norm. This requirement negates any potential efficiency gains, as the total runtime remains linearly dependent on κ .

Moreover, effective preconditioning, by definition, seeks to adjust the condition number of a problem. For preconditioners P_1 and P_2 to be effective, their total condition $\kappa(P_1)\kappa(P_2)$ must be close to $\kappa(S)$. Thus, attempting to apply classical matrix multiplication strategies, even those adapted for quantum computing, results in a significant subnormalization of the quantum state, proportional to $\kappa(S)$. This directly undermines the feasibility of straightforwardly applying classical preconditioning techniques in a quantum context, highlighting a key area where quantum computing diverges from classical computing paradigms.

Therein, a similar problem exists when considering the influence of machine precision on the accuracy of the result. First assembling all matrices and then using classical matrix preconditioning leads to a numerical error of the order of $\mathcal{O}(\kappa\epsilon)$, where ϵ is the machine precision. In contrast, directly assembling a discretization of $a(\mathcal{R}_1\bullet, \mathcal{R}_2\bullet)$ and $f^*(\mathcal{R}_1^*\bullet)$ – an approach called *full operator preconditioning* [MNUT24] – can avoid this dependence on κ . The same is possible on a quantum computer: by constructing a block encoding of $P_1 S P_2$ and the state $|P_1 r\rangle$ directly, rather than by multiplication with the preconditioner, the problems described above can be avoided.

For the right preconditioning, the computation of the solution as $c = P_2 y$ should also be avoided on quantum computers, while the measurement of $m^T c$ for a vector m may be feasible using the equivalence $m^T c = m^T P_2 y = (P_2^T m)^T y$. Consequently, we can obtain the result of a linear functional as long as we can efficiently construct $P_2^T m$. However, it is unclear how a quadratic quantity of interest of the form $\langle c | M | c \rangle$, otherwise popular in quantum computing, can be computed efficiently when nontrivial right preconditioning is used.

5.2. Optimal multilevel quantum preconditioning. The limitations highlighted above imply that a good preconditioner for quantum computing should result in a preconditioned matrix that is easy to construct directly, and not as a product of the system matrix and some preconditioner. The BPX preconditioner [BPX90] satisfies this requirement and is known to give a bounded condition number for the discrete Poisson-type problem (2.4)

independent of the refinement level L . Its usual formulation is

$$Pu = \sum_{\ell=1}^L \sum_{j=1}^{\dim \mathcal{V}_\ell} 2^{-\ell(2-d)} (u, \Lambda_j^{(\ell)})_{L^2} \Lambda_j^{(\ell)}.$$

Here we assume a hierarchical decomposition of \mathcal{V}_h based on the hierarchy of meshes $\mathcal{G}_1, \dots, \mathcal{G}_L$, where \mathcal{G}_ℓ corresponds to the Cartesian grid of width $h_\ell = 2^{-\ell}$ for $\ell = 1, \dots, L$ so that $\mathcal{G}_L = \mathcal{G}_h$ equals to the finest mesh. On each mesh we consider the Q1 finite element space $\mathcal{V}_\ell = \text{span}\{\Lambda_j^{(\ell)}\}_{j=1}^{\dim \mathcal{V}_\ell}$ spanned by the basis of hat functions $\Lambda_j^{(\ell)}$ associated with the interior vertices x_j of \mathcal{G}_ℓ . The symmetric preconditioning by P leads to a bounded condition number which is independent of the number of levels L .

Lemma 5.1 (Optimality of the BPX preconditioner). *Let $d \in \mathbb{N}, D \subset \mathbb{R}^d$ be a bounded domain and $\mathcal{V}_1 \subset \dots \subset \mathcal{V}_L \subset H_0^1(D)$ be finite element spaces. If, for all $1 \leq \ell \leq L$, these spaces fulfill the Jackson estimates*

$$\inf_{v_\ell \in \mathcal{V}_\ell} \|u - v_\ell\|_{L^2} \leq 2^{-\ell} C_1 \|u\|_{H^1}$$

for all $u \in H_0^1(D)$ and the Bernstein estimates

$$\|v_\ell\|_{H^1} \leq 2^\ell C_2 \|v_\ell\|_{L^2}$$

for all $v_\ell \in \mathcal{V}_\ell$ with constants $C_1, C_2 > 0$ independent of ℓ and L , then the condition of the symmetrically preconditioned stiffness matrix

$$\kappa(P^{1/2} S P^{1/2}) \in \mathcal{O}(1)$$

is bounded independent of L .

For a proof of this lemma we refer to [Osw90, DK92, Xu92]. Note that the constant hidden in the \mathcal{O} notation may grow with the dimension d . The sufficient conditions for the Lemma to hold are satisfied for our choice of uniformly refined grids and Q1 finite elements. The first assumption follows from the error estimate (2.6), and the second assumption is a consequence of the *inverse inequality* for polynomials.

In the classical context with the preconditioned conjugate gradient method, the explicit knowledge of $P^{1/2}$ is not required to apply symmetric preconditioning. No analogous argument is known for quantum computing. Since the non-symmetric left (or right) preconditioned system PS generally has no bounded condition number, we actually have to split the preconditioner P as is done for multilevel frames [Osw94, HW89] used in the context of finite element methods [Gri94b, Gri94a, HSS08]. For the split one considers the corresponding generating system

$$\mathcal{F} := \{f_{j,\ell} := 2^{-\ell(2-d)/2} \Lambda_j^{(\ell)} \mid 1 \leq \ell \leq L, 1 \leq j \leq \dim \mathcal{V}_\ell\}.$$

Let $P: \mathbb{R}^{|\mathcal{F}|} \rightarrow \mathcal{V}_L$ be the linear function given by

$$Fc = \sum_{\ell=1}^L \sum_{j=1}^{\dim \mathcal{V}_\ell} c_{j,\ell} f_{j,\ell}.$$

Then $P = FF^T$ can be written in terms of F [Osw94, Section 4.2.1] and we obtain the preconditioned system

$$(5.1) \quad F^T S F y = F^T r, \quad c = F y.$$

Note that F is not equal to $P^{1/2}$, since it is not symmetric or even square. Nevertheless, Lemma 5.1 serves as a bound on the condition number of (5.1), since the preconditioned matrix $F^T S F$ is spectrally equivalent to $P^{1/2} S P^{1/2}$ except for the non-trivial kernel, namely

$$\sigma(F^T S F) \setminus \sigma(P^{1/2} S P^{1/2}) = \{0\}.$$

Krylov methods in classical computers [Gri94b, Gri94a], as well as the quantum solvers based on quantum signal processing [GSLW19] or adiabatic quantum computing [AL22, LT20] that we intent to use, ignore the nontrivial kernel, so the effective condition of both systems is the same, and so is the effectiveness of the solvers.

6. QUANTUM REALIZATION OF THE FINITE ELEMENT METHOD

This section presents the main results of this paper, including a block encoding of the preconditioned stiffness matrix, optimal complexity bounds of the resulting quantum FEM, and an optimized quantum circuit realizing the method.

6.1. Implementation of the Preconditioned Stiffness Matrix. This section presents a quantum implementation of the preconditioned stiffness matrix $F^T S F$ from (5.1), which results from the finite element discretization of the partial differential equation (1.1) and BPX preconditioning. Since $F^T S F$ is not sparse in general, this is a nontrivial task where standard techniques are not applicable. Instead, we will make heavy use of Proposition 3.5 to decompose the preconditioned system into sums, products, and tensor products of smaller matrices with an explicit encoding.

First, we will treat the problem for general domains D , reducing it to the construction of matrices representing finite element gradients independent of the diffusion coefficient A and grid transfer operators encoding a hierarchical grid structure. Under the assumption, that block encodings of these matrices are provided with bounded subnormalization, we will check using the bounds given in Proposition 3.5 that the total subnormalization of the construction is bounded. We will then give an explicit implementation of the structural matrices for the case of uniform Cartesian grids on the unit cube.

In addition to the continuous finite element spaces \mathcal{V}_ℓ our construction relies on the auxiliary spaces of discontinuous Q1 elements $\mathcal{Q}_\ell \supset \mathcal{V}_\ell$ on \mathcal{G}_ℓ . For these spaces of dimension $2^{d(\ell+1)}$, L^2 -orthonormal bases are composed of 2^d local basis functions $\psi_{j,1}^{(\ell)}, \dots, \psi_{j,2^d}^{(\ell)}$ per grid cell $G_j \in \mathcal{G}_\ell$, $1 \leq j \leq 2^{d\ell}$. Our decomposition relies on the matrix representations C_ℓ of size $d2^{d(\ell+1)} \times (2^\ell - 1)^d$ of the gradient $\nabla: \mathcal{V}_\ell \rightarrow \mathcal{Q}_\ell^d$ acting on finite element spaces. Furthermore, we need the $2^{d(L+1)} \times 2^{d(\ell+1)}$ transfer matrices $T_{\ell,L}$ representing the inclusion $\mathcal{Q}_\ell \rightarrow \mathcal{Q}_L$. The vector valued space $\mathcal{Q}_\ell^d = \mathcal{Q}_\ell \otimes \mathbb{R}^d$ has an orthonormal basis with basis vectors $\psi_{j,k}^{(l)} \otimes e_s$ where e_s is the s -th standard basis vector.

Remark 6.1 (Qubit register ordering). We assume a special encoding of the spaces \mathcal{Q}_ℓ and \mathcal{V}_ℓ in qubit registers. Specifically, the basis function $\Lambda_j^{(\ell)} \in \mathcal{V}_\ell$ should be represented (ignoring ancilla registers) by the integer of its index $|j\rangle$, the basis function $\psi_{j,k}^{(\ell)} \in \mathcal{Q}_\ell$ by $|j\rangle |k\rangle$ and $\psi_{j,k}^{(l)} \otimes e_s$ should be represented by $|j\rangle |s\rangle |k\rangle$. For some block encodings we will need a different order of qubit registers, which corresponds to a permutation π of rows and columns of the encoded matrix. The permutation π is unitary and a block encoding is given by a number of SWAP instructions that change the order of qubits correspondingly.

The following theorem constructs an abstract block encoding of the preconditioned matrix $F^T S F$ if the matrices C_ℓ and $T_{\ell,L}$ are provided as block encodings U_{C_ℓ} and $U_{T_{\ell,L}}$ in the sense of Definition 3.3 and the diffusion coefficient A is given in the format U_A of Proposition 3.6.

Theorem 6.2 (Block encoding of preconditioned stiffness matrix). *Let $L \in \mathbb{N}$ and U_{C_ℓ} and $U_{T_{\ell,L}}$ be block encodings of the finite element gradient C_ℓ and transfer matrices $T_{\ell,L}$ for $1 \leq \ell \leq L$ respectively. Let additionally U_A be a quantum circuit that computes the value of the diffusion coefficient A . We can then construct a block encoding of the matrix $F^T S F$ with subnormalization less than*

$$\frac{\beta}{\alpha} \sum_{\ell=1}^L (\tilde{\gamma}(U_{C_\ell}) \tilde{\gamma}(U_{T_{\ell,L}}))^2$$

with α and β defined in (2.2) and normalization

$$\beta \sum_{\ell=1}^L 2^{-\ell(2-d)} (\gamma(U_{C_\ell}) \gamma(U_{T_{\ell,L}}))^2.$$

Proof. Due to the choice of an orthonormal basis, the L^2 inner product of two \mathcal{Q}_L functions is equal to the Euclidean inner product of their coefficients in basis representations. Recall that we assume the diffusion coefficient A to be constant on the cells meaning under the chosen basis it corresponds to a block diagonal matrix D_A with the $d \times d$ blocks $(D_A)_{jj} = A|_{T_j}$ representing the diffusion coefficient in the j -th grid cell $G_j^L \in \mathcal{G}_L$. We thus obtain a decomposition

$$(6.1) \quad S = C_L^T (D_A \otimes \text{Id}_{2^d}) C_L$$

of the stiffness matrix. Using Proposition 3.6, the block diagonal matrix D_A can be realized efficiently on a quantum computer. The decomposition (6.1) gives rise to a decomposition of the preconditioned system

$$(6.2) \quad F^T S F = C_F^T (D_A \otimes \text{Id}_{2^d}) C_F$$

with $C_F = C_L F$. The factors C_L and F of C_F are not well conditioned, so we can not gain an efficient implementation of C_F using just (3.2d). Still we can decompose this matrix further by using the hierarchical structure induced by the preconditioner. The blocks of F correspond up to scalar factor to the inclusions $\mathcal{V}_\ell \rightarrow \mathcal{V}_L$ for $1 \leq \ell \leq L$. It follows that C_F also has a $1 \times L$ block structure where the ℓ -th block for $1 \leq \ell \leq L$ corresponds to the gradient on the level ℓ , specifically the function $\nabla: \mathcal{V}_\ell \rightarrow \mathcal{Q}_L^d$, scaled by a factor of $2^{-\ell(2-d)/2}$. This factors through \mathcal{Q}_ℓ^d , which can be seen from the following commutative diagram:

$$\begin{array}{ccc} \mathcal{V}_\ell & \xrightarrow{F|_{\mathcal{V}_\ell}} & \mathcal{V}_L \\ 2^{-\ell(2-d)/2} C_\ell \downarrow & & \downarrow C_L \\ \mathcal{Q}_\ell^d & \xrightarrow{\tilde{T}_{\ell,L}} & \mathcal{Q}_L^d \end{array}$$

The matrix for the inclusion of the vector valued function spaces $\mathcal{Q}_\ell^d \hookrightarrow \mathcal{Q}_L^d$ is given by

$$\tilde{T}_{\ell,L} := \pi^T (\text{Id}_d \otimes T_{\ell,L}) \pi$$

where π is the permutation of qubits $|j\rangle|s\rangle|k\rangle \mapsto |s\rangle|j\rangle|k\rangle$, see also Remark 6.1. With this we can write

$$C_F = \begin{bmatrix} 2^{-(2-d)/2} \tilde{T}_{1,L} C_1 & \dots & 2^{-\ell(2-d)/2} \tilde{T}_{\ell,L} C_\ell & \dots & 2^{-L(2-d)/2} \tilde{T}_{L,L} C_L \end{bmatrix}$$

We would now like to estimate the subnormalization of the construction. First note that the mapping $\mathcal{Q}_\ell \hookrightarrow \mathcal{Q}_L$ preserves the L^2 product, and as under the chosen bases of both \mathcal{Q}_ℓ and \mathcal{Q}_L this is equal to the Euclidean inner product we can deduce that the columns of $T_{\ell,L}$ are orthonormal. This means that the matrices are perfectly conditioned, i.e.

$$\kappa(T_{\ell,L}) = \kappa(\tilde{T}_{\ell,L}) = 1.$$

As such we can use (3.2d) and (3.2e) of Proposition 3.5 to see that the block encoding of C_F has subnormalization

$$\tilde{\gamma}(C_F) = \left(\sum_{\ell=1}^L (\tilde{\gamma}(U_{C_\ell}) \tilde{\gamma}(U_{T_{\ell,L}}))^2 \right)^{1/2}.$$

The statement for the normalization then follows from using (3.2d) of Proposition 3.5 again on the factorization (6.2). For the bound of the subnormalization we use

$$|F^T S F| = |C_F^T (D_A \otimes \text{Id}_{2^d}) C_F| = |(D_A^{1/2} \otimes \text{Id}_{2^d}) C_F|^2 \geq \kappa(D_A^{1/2})^{-2} |D_A^{1/2}|^2 |C_F|^2.$$

Note that the symmetric decomposition of $D_A^{1/2}$ is only for theoretical purposes and is not needed for the quantum computation. The subnormalization can then be estimated as

$$\begin{aligned} \tilde{\gamma}(C_F^T (D_A \otimes \text{Id}_{2^d}) C_F) &= \frac{\gamma(C_F^T (D_A \otimes \text{Id}_{2^d}) C_F)}{|C_F^T (D_A \otimes \text{Id}_{2^d}) C_F|} \\ &\leq \frac{\kappa(D_A) \gamma(D_A) \gamma(C_F)^2}{|D_A| |C_F|^2} = \kappa(D_A) \tilde{\gamma}(D_A) \tilde{\gamma}(C_F)^2 \leq \frac{\beta}{\alpha} \tilde{\gamma}(C_F)^2. \quad \square \end{aligned}$$

We emphasise that the coefficient A does not have to conform to any special structure, like being tensorial in the spatial dimensions, in order for such an implementation to be possible.

Example 6.3 (Non-tensorial coefficient). Consider for $d = 2$ the coefficient $A(x_1, x_2) = \sqrt{1 + x_1 + x_2}$ which can clearly be computed to accuracy tol in almost constant time $\mathcal{O}(\log \text{tol})$. Still this cannot be written as a decomposition of the form

$$A(x_1, x_2) = A_1(x_1) \cdot A_2(x_2)$$

We could even consider a function $A_k: \{1, \dots, 2^{dL}\} \rightarrow [\alpha, \beta]$ that acts as a pseudorandom number generator, i.e. for a random key k it is almost indistinguishable from random.

Up until now the treatment of the implementation was independent of the domain D , however implementing the matrices $T_{\ell,L}$ and C_ℓ now strongly depends on the structure of the mesh. As such we will now again consider the simplest case of a uniform grid on the d -dimensional cube $[0, 1]^d$. The same approach should work for more general meshes however, see also Remark 6.5.

Theorem 6.4 (Block encoding of preconditioned stiffness matrix on Cartesian grids). *Let $L, d \in \mathbb{N}$, $D := [0, 1]^d$ and \mathcal{G}_L be the regular grid on D . We can then construct a block encoding of $F^T S F$ with subnormalization $\frac{\beta}{\alpha} dL$ and normalization $\beta 2^{d+1} dL$.*

Proof. For our construction we will use the tensorial structure of the problem, namely that the spaces \mathcal{V}_ℓ and \mathcal{Q}_ℓ can be decomposed as

$$(6.3) \quad \mathcal{V}_\ell = \mathcal{V}_{\ell,1D}^{\otimes d} \quad \text{and} \quad \mathcal{Q}_\ell = \mathcal{Q}_{\ell,1D}^{\otimes d}$$

where $\mathcal{V}_{\ell,1D}$ and $\mathcal{Q}_{\ell,1D}$ are the finite elements spaces of P1 and discontinuous P1 finite elements on the one-dimensional domain $[0, 1]$ with cells of width $2^{-\ell}$. In terms of the encoding of \mathcal{V}_ℓ and \mathcal{Q}_ℓ given in Remark 6.1 this means that the register corresponding to the spatial index $1 \leq j \leq 2^{d\ell}$ is decomposed into registers storing the index in each of the spatial dimensions

$$|j\rangle = |j_1\rangle \dots |j_d\rangle.$$

Similarly for a basis function $\psi_{j,k}^{(\ell)} \in \mathcal{Q}_\ell$ the index $1 \leq k \leq 2^d$ is decomposed into d 1-qubit registers

$$|k\rangle = |k_1\rangle \dots |k_d\rangle.$$

To use Proposition 6.2 we now have to choose an orthonormal basis of \mathcal{Q}_ℓ and we do so by choosing a basis on $\mathcal{Q}_{\ell,1D}$. For this consider the functions $\psi_0(x) = 1$ and $\psi_1(x) = 2\sqrt{3}x - \sqrt{3}$ on the reference cell $[0, 1]$. One can check that these are indeed orthonormal. For $1 \leq j \leq 2^\ell$ let ϕ_j be the linear mapping from $[0, 1]$ to $[(j-1)2^{-\ell}, j2^{-\ell}]$. Then $(2^{\ell/2}\phi_j\psi_k)_{1 \leq j \leq 2^\ell, k=0,1}$ is an orthonormal basis of $\mathcal{Q}_{\ell,1D}$. This induces an orthonormal basis of \mathcal{Q}_ℓ through the relation (6.3). With this choice of basis we also introduce one-dimensional equivalents of relevant matrices. Specifically for $1 \leq \ell \leq L$ we write $T_{\ell,k,1D}$ for the $2^{\ell+1} \times 2^{k+1}$ matrix encoding the inclusion $\mathcal{Q}_{\ell,1D} \subset \mathcal{Q}_{k,1D}$ and we extend this definition to $\ell \leq k \leq L$. Further we define $C_{\ell,1D}$ and $R_{\ell,1D}$ as the $2^{\ell+1} \times 2^\ell - 1$ matrices encoding the derivative $\partial_1: \mathcal{V}_{\ell,1D} \rightarrow \mathcal{Q}_{\ell,1D}$ and the inclusion $\mathcal{V}_{\ell,1D} \subset \mathcal{Q}_{\ell,1D}$. To conform to our assumption in Remark 6.1 on the ordering of basis elements the induced basis of \mathcal{Q}_ℓ needs a slight reordering by permutation

$$\pi_\ell: |j_1\rangle \dots |j_d\rangle |k_1\rangle \dots |k_d\rangle \mapsto |j_1\rangle |k_1\rangle \dots |j_d\rangle |k_d\rangle$$

which groups the indices belonging to one dimension together.

In addition to the tensor structure of the function spaces we also obtain a tensor structure of the gradient since

$$(\nabla v)_s = \partial_s v = \underbrace{\text{Id} \otimes \dots \otimes \text{Id}}_{s-1} \otimes \partial_1 \otimes \underbrace{\text{Id} \otimes \dots \otimes \text{Id}}_{d-s}$$

for $1 \leq s \leq d$. On the matrix level this means that $\pi_\ell C_\ell$ is a $d \times 1$ block matrix, where the s -th block is given by

$$\underbrace{R_{\ell,1D} \otimes \dots \otimes R_{\ell,1D}}_{s-1} \otimes C_{\ell,1D} \otimes \underbrace{R_{\ell,1D} \otimes \dots \otimes R_{\ell,1D}}_{d-s}$$

Additionally the matrices $R_{\ell,1D}$ and $C_{\ell,1D}$ can be given explicitly:

$$2^{\ell/2} R_{\ell,1D} = \begin{bmatrix} \frac{1}{2} & \frac{1}{2} \\ \frac{1}{2\sqrt{3}} & -\frac{1}{2\sqrt{3}} \end{bmatrix} \begin{bmatrix} I_\ell \\ N_\ell \end{bmatrix} \quad \text{and} \quad 2^{-\ell/2} C_{\ell,1D} = \begin{bmatrix} 1 & -1 \\ 0 & 0 \end{bmatrix} \begin{bmatrix} I_\ell \\ N_\ell \end{bmatrix}.$$

where $I_\ell = \text{Id}_{2^\ell, 2^\ell-1}$ and $N_\ell \in \mathbb{R}^{2^\ell \times 2^\ell-1}$ is the matrix of the mapping $|k\rangle \mapsto |k+1\rangle$, in other words

$$N_\ell := \begin{bmatrix} 0 & \dots & \dots & 0 \\ 1 & 0 & & \vdots \\ 0 & 1 & \ddots & \vdots \\ \vdots & \ddots & \ddots & 0 \\ 0 & \dots & 0 & 1 \end{bmatrix}$$

Block encodings of both N_ℓ and I_ℓ can be implemented, even without the use of extra ancilla qubits. For addition see for example [Dra00]. Note that the block matrix $[I_\ell \ N_\ell]^T$ has orthonormal columns and as such condition number 1. Similarly the 2×2 coefficient matrices can be implemented without subnormalization since they are of constant size. This means that the block encodings for $R_{\ell,1D}$ and $C_{\ell,1D}$ have no subnormalization. Using (3.2e) of Proposition 3.5 it then follows that the rescaled matrix $2^{-\ell(2-d)/2}C_\ell$ can be implemented with subnormalization at most \sqrt{d} . Similarly one can check that the encoding for $2^{\ell/2}R_{\ell,1D}$ has a normalization of $\sqrt{2}$ while the encoding for $2^{\ell/2}C_{\ell,1D}$ has a normalization of 2 leading to a normalization of $2^{-\ell(2-d)/2}C_\ell$ by $2^{(d+1)/2}$.

Finally the matrices $T_{\ell,L}$ can also be factorized. Again due to (6.3) we get the property $\pi_L T_{\ell,L} \pi_\ell^T = T_{\ell,L,1D}^{\otimes d}$. This can be further decomposed as $\mathcal{Q}_{\ell,1D} \hookrightarrow \mathcal{Q}_{\ell+1,1D} \hookrightarrow \dots \hookrightarrow \mathcal{Q}_{L,1D}$ or in other words

$$\pi_L T_{\ell,L} \pi_\ell^T = (T_{L-1,L,1D} \dots T_{\ell,\ell+1,1D})^{\otimes d}$$

The matrices $T_{\ell,\ell+1,1D}$ are explicitly given by

$$T_{\ell,\ell+1,1D} = \text{Id}_{2^\ell} \otimes \frac{1}{\sqrt{2}} \begin{bmatrix} 1 & -\sqrt{3}/2 \\ 0 & 1/2 \\ 1 & \sqrt{3}/2 \\ 0 & 1/2 \end{bmatrix}$$

which has orthonormal columns and as such a condition number of 1. This means $T_{\ell,L}$ has condition number 1 and the block encoding has normalization and subnormalization 1. The claim follows by Proposition 6.2. \square

Remark 6.5. Our technique can easily be adapted to domains $D \subset [0, 1]^d$ such that D is a union of cells on some level ℓ_0 . This is because the matrices $T_{\ell,L}$ and C_ℓ for $\ell_0 \leq \ell \leq L$ are obtained from the ones defined in Proposition 6.4 by a simple projection. We would need to truncate the hierarchical sequence of meshes at ℓ_0 , meaning that the condition number would not be independent of ℓ_0 .

6.2. Complexity of quantum FEM. We will now comment on the complete algorithm and measurement procedure. As stated earlier, because of the symmetric preconditioning it is not possible to measure quantities of interest of the form $\langle c | M | c \rangle$, but rather the goal should be computing a linear functional of the solution, in other words $m^T c$.

Theorem 6.6 (Complexity of quantum FEM). *Let $\text{tol} > 0$, $d \in \mathbb{N}$, $D = [0, 1]^d$, and $\kappa_d := \kappa(F^T S F)$. Let U_r and U_m be quantum circuits that construct the normalized states corresponding to the right hand side and quantity of interest, as outlined in Appendix A. Additionally let U_A be a quantum circuit that computes the value of the coefficient as*

defined in 3.6. Then the quantity of interest can be computed as the phase of a qubit up to accuracy tol using $\mathcal{O}(\sqrt{\kappa_d} \text{poly log}(\kappa_d \text{tol}^{-1}))$ uses of U_r , U_m , $\mathcal{O}(1)$ uses of U_A , and $\mathcal{O}(\sqrt{\kappa_d} \text{poly log}(\kappa_d \text{tol}^{-1}))$ additional gates. To measure the phase, the algorithm is repeated $\mathcal{O}(\text{tol}^{-1})$ times leading to a total runtime of $\mathcal{O}(\sqrt{\kappa_d} \text{tol}^{-1} \text{poly log}(\kappa_d \text{tol}^{-1}))$.

Proof. We decompose the linear system as described in Propositions 6.2 and 6.4, specifically in the form of

$$F^T S F = C_F^T (D_A \otimes \text{Id}) C_F$$

by which we also get block encodings for all factors. Inserting the definition of the solution c and using the decomposition from Proposition 6.2 we obtain

$$m^T c = m^T (F^T S F)^{-1} r = (C_F^+ m)^T (D_A^{-1} \otimes \text{Id}) C_F^+ r$$

and by Lemma 5.1 we know $\kappa(C_F) \in \mathcal{O}(\sqrt{\kappa(F^T S F)}) = \mathcal{O}(\sqrt{\kappa_d})$. As such we can first compute the least square solutions $C_F^+ m$ and $C_F^+ r$ in parallel, which takes

$$\mathcal{O}(\sqrt{\kappa_d} \text{poly log}(\kappa_d \text{tol}^{-1}))$$

uses of either oracles U_r and U_m and a proportional number of additional operations following Theorem 4.2. We then measure with the matrix D_A^{-1} . Depending on the information one has on the coefficient a block encoding for this matrix can either be computed directly or using a quantum linear system algorithm. This procedure gives a roughly quadratic improvement in runtime over simply computing the solution $|c\rangle$ and measuring using a swap test. Equivalently we consider the block system

$$\begin{bmatrix} C_F D_A^{1/2} & 0 \\ 0 & C_F D_A^{1/2} \end{bmatrix} \begin{bmatrix} y \\ y' \end{bmatrix} = \begin{bmatrix} F^T r \\ F^T m \end{bmatrix}$$

where the block encoding of the left hand side matrix $\text{Id} \otimes (C_F D_A^{1/2})$ only requires one call to the block encoding of C_F . We can then measure

$$\begin{bmatrix} y \\ y' \end{bmatrix}^T \begin{bmatrix} 0 & \text{Id} \\ \text{Id} & 0 \end{bmatrix} \begin{bmatrix} y \\ y' \end{bmatrix}$$

using the Hadamard test [AJL06]. This approach is similar to the ‘‘Modified Hadamard test’’ described in [Luo20]. This can be either done using $\mathcal{O}(\text{tol}^{-2})$ separate runs of the algorithm or using phase estimation [Kit95, Lin22] in runtime $\mathcal{O}(\text{tol}^{-1})$. The complete circuit can be seen in Figure 6.1. □

Remark 6.7 (Measurement procedure). To achieve the claimed optimal runtime of

$$\mathcal{O}(\text{tol}^{-1} \text{poly log tol}^{-1}),$$

one must use phase estimation [Kit95, Lin22] as a measurement technique. For this, the circuit must be applied a number of times proportional to tol^{-1} within a coherent run. This would mean that the depth of the whole quantum circuit scales linearly with tol^{-1} , which leads to a worse dependence on the noise of the quantum computer. Alternatively, one can use a typical Monte Carlo approach to estimate the output probabilities. This leads to a worse dependence of the runtime on tol^{-1} , namely a total runtime of $\mathcal{O}(\text{tol}^{-2} \text{poly log tol}^{-1})$. However, the depth of the entire quantum circuit scales only

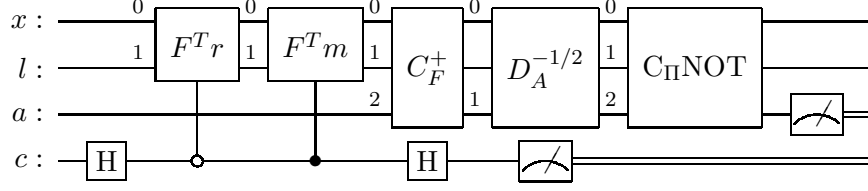


FIGURE 6.1. Implementation of an efficient algorithm to compute the quantity of interest $m^T S^{-1} r$, which can be computed as $P(a = 0, c = 0) - P(a = 0, c = 1)$.

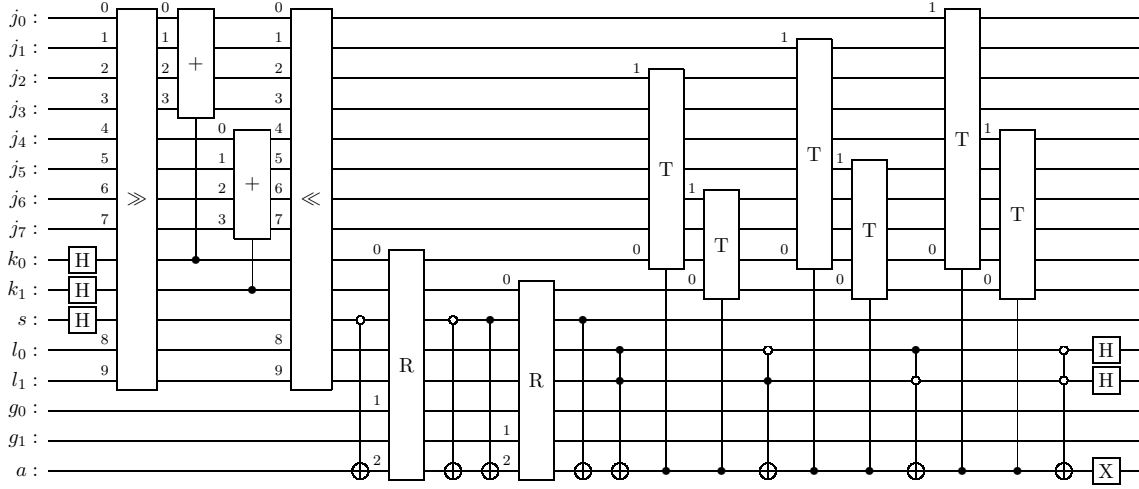
logarithmically with tol^{-1} , which makes the algorithm less sensitive to noise in the quantum computer. These considerations are not unique to our method, but appear in any approach that uses the Hadamard or swap test [AJL06, BCWDW01] as a measurement procedure.

Remark 6.8 (Dependence on d). Note that the condition number κ_d of the preconditioned finite element system may depend in a critical way on the dimension d [Bac23, Remark 3.2.]. To the best of our knowledge the asymptotic behaviour of the BPX preconditioner has not been analyzed with regard to its dependence on d as $d \rightarrow \infty$. The best bound for the unpreconditioned system known to us is exponential in d , but we do not see this behaviour in numerical experiments with low dimension. If the condition instead depends only polynomially on the dimension, then our scheme would give an exponential speedup with respect to d over classical methods, specifically an asymptotic runtime of $\mathcal{O}(\text{tol}^{-1} \text{poly}(d \log \text{tol}^{-1}))$.

6.3. Optimized quantum circuit. We turn now to our actual implementation of the block encoding for C_F . Indeed this could be done using the operations of Proposition 3.5 and their concrete implementations in Appendix B, but this will lead to a large overhead which can mostly be attributed to two reasons: first the inner projection in the multiplication (see Figure B.1) can be avoided in some cases and with our implementation none of these projections are needed at all. And second there is often a more efficient way to implement block matrices than to use controlled applications of the blocks. Consider for example the block matrix

$$\begin{bmatrix} I_L & N_L & I_{L-1} & \dots & N_1 \end{bmatrix}^T$$

which arises from the construction of Proposition 6.4. The 2ℓ -th block for $1 \leq \ell \leq L$ are simply encoded by identity, while the $(2\ell + 1)$ -th block is implemented by incrementing of the integer encoded in the $(L - \ell)$ highest bits of the work register or equivalently by first shifting the bits of the work register right by ℓ bits, then incrementing the complete work register, and then shifting the work register left again by ℓ bits. With the latter procedure all incrementing operations overlap and only one such subcircuit is needed. A similar technique is used to compress the circuit implementing the matrices $T_{\ell,L}$. An overview of the complete quantum circuit is given in Figure 6.2. The gates denoted with R are related to the implementation of $R_{\ell,1D}$ and $C_{\ell,1D}$, while the ones denoted with T are related to the implementation of $T_{\ell,\ell+1,1D}$ from Proposition 6.4. For technical details we

FIGURE 6.2. Block encoding (without $C_{\Pi}\text{NOT}$) of C_F for $d = 2$ and $L = 4$

refer to our complete Qiskit implementation available at <https://github.com/MDeiml/quantum-bpx>.

7. NUMERICAL EXPERIMENT

In this section, we validate the quantum circuit proposed above using first a noiseless quantum simulator. We then analyze the dependence of our algorithm on realistic noise, which is unavoidable in real quantum computers, and address the viability of practical use of our method.

The experiments use the Quantum Singular Value Transformation (QSVT) [GSLW19] to compute the pseudoinverse C_F^+ . Although the runtime of this method scales quadratically in κ it is very efficient in the well-conditioned regime which we consider here. The QSVT works by transforming the initial state $|\tilde{r}\rangle := F^T r$ by a polynomial p of the input matrix C_F , in other words one can produce the state $p(C_F)|\tilde{r}\rangle$. Among other conditions, the polynomial must satisfy $|p(z)| \leq 1$ for $z \in [-1, 1]$. The QSVT aims to approximate the function $g(z) = 1/z$ on the domain $[-1, -\kappa] \cup [\kappa, 1]$ using p , since $g(C_F) = C_F^+$ is the pseudoinverse of C_F . Following the construction in [GSLW19], an approximation is realized by the polynomial

$$\tilde{p}(z) = 4 \sum_{j=0}^J (-1)^j \frac{\sum_{k=j+1}^K \binom{2K}{K+k}}{2^{2K}} t_{2j+1}(z),$$

where t_{2j+1} is the Chebyshev polynomial of degree $2j+1$, $j = 0, \dots, J$, and the parameter $J, K \in \mathbb{N}$ can be chosen appropriately given κ and the error tolerance tol . Specifically, [GSLW19] shows the choices

$$K = \lceil \kappa^2 \log(\kappa \text{tol}^{-1}) \rceil \quad \text{and} \quad J = \left\lceil \sqrt{K \log(4K \text{tol}^{-1})} \right\rceil$$

lead to optimal error bounds. The polynomial \tilde{p} is then normalized to not exceed the range $[-1, 1]$, resulting in the final polynomial p . For the purpose of the QSVT, this polynomial

p is translated into so-called *phase angles*, which we compute using the software `pyqsp` [MRTC21]. For details see [GSLW19, MRTC21].

We implement the circuit of Section 6.3 and Theorem 6.6 in the simulation framework Qiskit [Qis23] to validate its correctness. The source code is available at <https://github.com/MDeiml/quantum-bpx>. Indeed the simulation results show that the quantum circuit encodes the intended finite element stiffness matrix with machine accuracy. We can also see that the resulting transpiled circuits are quite compact, with the block encoding of C_F including both C_{Π} NOT operations requiring only 13 qubits and 300 two-qubit gates for $d = 1$ and $L = 4$. Thus, the complete circuit for estimating a quantity of interest requires about $300(2J + 1)$ two-qubit gates (ignoring the gates needed to encode the right-hand side).

From these observations, one can estimate the expected error on a quantum computer with realistic noise. Since this noise-induced error is dominated by the error of using two-qubit gates ϵ_2 [MBA⁺23], a very rough estimate gives the error as $\varepsilon \approx 300(2J + 1)\epsilon_2$. Equivalently, to obtain a prescribed error of $\varepsilon > 0$, the two-qubit error must be at most $\epsilon_2 \lesssim \varepsilon/(300(2J + 1))$. For an error of $\varepsilon = 0.1$ this gives $\epsilon_2 < 3.3 \cdot 10^{-4}/(2J + 1)$. This does not take into account the various error mitigation and error correction methods that already exist [DMN13, CBB⁺23] or any future improvements to such methods. For comparison, current state of the art quantum computers achieve a two-qubit error rate of $\epsilon_2 \approx 1.8 \cdot 10^{-3}$ [MBA⁺23], meaning that a further hardware improvement of about one order of magnitude is needed to make our approach practical. Nevertheless, this shows the competitiveness of the proposed approach in the near future.

To back up this assessment with a numerical experiment, we simulate our algorithm with $d = 1$ and $L = 4$ on a noisy quantum simulator for different levels of noise. We choose the model data $A \equiv 1$ and $f \equiv 1$, which implies $r = 2^{-4}(1, \dots, 1)^T$. We measure the Galerkin finite element approximation using the vector $m = |8\rangle = (\delta_{js})_{1 \leq j \leq 15}$, which gives us the calculated value of the quantum algorithm at the node $x = \frac{9}{16}$. We run this experiment with a two-qubit error ranging from 10^{-2} to 10^{-6} as well as noise for one-qubit gates scaled 10^{-2} times the two-qubit error. For each data point we compute 200 runs to estimate a 95% confidence interval of the predicted quantum solution. Each run contains 1000 measurement samples. The results can be seen in Figure 7.1. There, the gray line indicates the value of the true finite element solution on the uniform mesh of width $h = 2^{-L}$, which coincides with the exact solution of the PDE [MP20, Chapter 2], namely $u(\frac{9}{16}) = \frac{63}{512}$. While the error of the QSVT is too high for $J = 4$, the results for $J = 5$ and $J = 12$ indicate reasonable convergence to the true solution of the linear system for increasing J . Note, however, that this comes with an increasing error due to noise, with $J = 12$ converging the slowest.

For comparison, the plot also includes the result of the same measurement procedure without noise. This data point shows roughly the same confidence interval, meaning that the uncertainty in the other results is largely due to the sampling procedure associated with the measurement rather than the noise. For uncertainties due to noise, we would expect the confidence interval to grow with increasing error, but this is not true except for the rightmost points with $J = 12$. Instead, the increasing noise seems to cause a bias away from the true solution.

These results nicely show that with the moderate choice of $J = 5$ one could obtain an estimate of the quantity of interest within a relative error of about 0.1 given a quantum computer with a two-qubit error of 10^{-4} , supporting our prediction above. A relative error

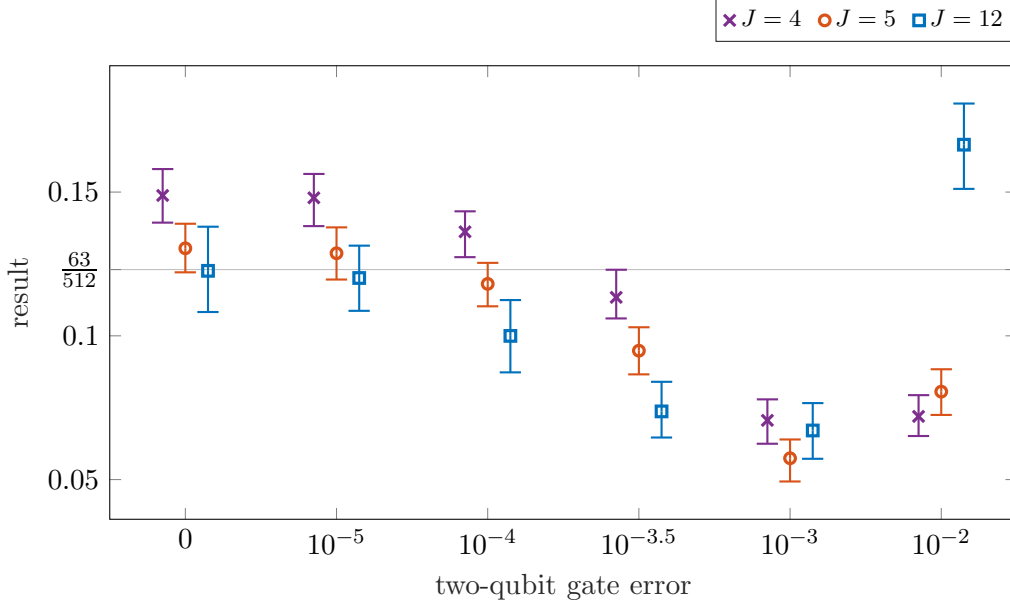


FIGURE 7.1. The results for noisy simulation of the algorithm with $J = 4, 5, 12$. The gray line corresponds to the true value of the PDE solution. The markers are the empirical expectation of the runs while the bars indicate a confidence interval of 95%.

of 0.01 is instead achieved with $J = 12$, but this would require a quantum computer with a two-qubit error of 10^{-5} . Note, however, that these results are inconclusive because our simulations ignore other sources of error in real quantum computers, such as measurement or increased circuit size due to limited qubit connectivity.

8. CONCLUSION

In this research article, we have demonstrated the feasibility of the finite element method for quantum computing, achieving a significant speedup by optimizing the runtime of our proposed algorithm through the integration of the well-established BPX preconditioner. The method not only realizes optimal performance in terms of the error tolerance – a prospect previously only theorized [MP16] – but is also characterized by its low quantum circuit depth, bringing it excitingly close to the abilities of real quantum computers.

However, one aspect that remains to be fully explored is how the efficiency of the algorithm is affected by high dimensions. While this question will hopefully be answered empirically on real quantum computers in the not too distant future, its mathematical understanding requires novel and refined techniques of numerical analysis to obtain dimension-robust condition number estimates of preconditioned finite element discretizations, which have so far been explored up to dimension three or accepting exponentially growing dimension dependencies. Therefore, future work should aim to elucidate the scalability of our algorithm to high dimensions, potentially opening new frontiers in the application of quantum computing to complex problem solving.

REFERENCES

- [AJL06] D. Aharonov, V. Jones, and Z. Landau. A polynomial quantum algorithm for approximating the jones polynomial. In *Proceedings of the thirty-eighth annual ACM symposium on Theory of computing*, pages 427–436, 2006.
- [AL22] D. An and L. Lin. Quantum linear system solver based on time-optimal adiabatic quantum computing and quantum approximate optimization algorithm. *ACM Transactions on Quantum Computing*, 3(2):1–28, June 2022.
- [Amb10] A. Ambainis. Variable time amplitude amplification and a faster quantum algorithm for solving systems of linear equations. *arXiv preprint arXiv:1010.4458*, 2010.
- [Bac23] M. Bachmayr. Low-rank tensor methods for partial differential equations. *Acta Numerica*, 32:1–121, May 2023.
- [BCK15] D. W. Berry, A. M. Childs, and R. Kothari. Hamiltonian simulation with nearly optimal dependence on all parameters. In *2015 IEEE 56th annual symposium on foundations of computer science*, pages 792–809. IEEE, 2015.
- [BCOW17] D. W. Berry, A. M. Childs, A. Ostrander, and G. Wang. Quantum algorithm for linear differential equations with exponentially improved dependence on precision. *Communications in Mathematical Physics*, 356(3):1057–1081, December 2017.
- [BCWDW01] H. Buhrman, R. Cleve, J. Watrous, and R. De Wolf. Quantum fingerprinting. *Physical Review Letters*, 87(16):167902, September 2001.
- [Ber14] D. W. Berry. High-order quantum algorithm for solving linear differential equations. *Journal of Physics A: Mathematical and Theoretical*, 47(10):105301, March 2014.
- [BG04] H. Bungartz and M. Griebel. Sparse grids. *Acta Numerica*, 13:147–269, May 2004.
- [BH97] G. Brassard and P. Hoyer. An exact quantum polynomial-time algorithm for simon’s problem. In *Proceedings of the Fifth Israeli Symposium on Theory of Computing and Systems*, pages 12–23. IEEE, 1997.
- [BK20] M. Bachmayr and V. Kazeev. Stability of Low-Rank Tensor Representations and Structured Multilevel Preconditioning for Elliptic PDEs. *Foundations of Computational Mathematics*, 20(5):1175–1236, October 2020.
- [BNWAG23] M. Bagherimehrab, K. Nakaji, N. Wiebe, and A. Aspuru-Guzik. Fast quantum algorithm for differential equations. *arXiv preprint arXiv:2306.11802*, 2023.
- [BPX90] J. H. Bramble, J. E. Pasciak, and J. Xu. Parallel multilevel preconditioners. *Math. Comp.*, 55(191):1–22, 1990.
- [BS08] S. C. Brenner and L. R. Scott. *The mathematical theory of finite element methods*, volume 15 of *Texts in Applied Mathematics*. Springer, New York, third edition, 2008.
- [CBB⁺23] Z. Cai, R. Babbush, S. C. Benjamin, S. Endo, W. J. Huggins, Y. Li, J. R. McClean, and T. E. O’Brien. Quantum error mitigation. *Reviews of Modern Physics*, 95(4):045005, 2023.
- [CJS13] B. D. Clader, B. C. Jacobs, and C. R. Sprouse. Preconditioned quantum linear system algorithm. *Physical Review Letters*, 110(25):250504, June 2013.
- [CKS17] A. M. Childs, R. Kothari, and R. D. Somma. Quantum Algorithm for Systems of Linear Equations with Exponentially Improved Dependence on Precision. *SIAM Journal on Computing*, 46(6):1920–1950, January 2017.
- [CL20] A. M. Childs and J. Liu. Quantum spectral methods for differential equations. *Communications in Mathematical Physics*, 375(2):1427–1457, April 2020.
- [CLO21] A. M. Childs, J. Liu, and A. Ostrander. High-precision quantum algorithms for partial differential equations. *Quantum*, 5:574, November 2021.
- [CPP⁺13] Y. Cao, A. Papageorgiou, I. Petras, J. Traub, and S. Kais. Quantum algorithm and circuit design solving the Poisson equation. *New Journal of Physics*, 15(1):013021, January 2013.
- [DK92] W. Dahmen and A. Kunoth. Multilevel preconditioning. *Numerische Mathematik*, 63(1):315–344, December 1992.
- [DMN13] S. J. Devitt, W. J. Munro, and K. Nemoto. Quantum error correction for beginners. *Reports on Progress in Physics*, 76(7):076001, 2013.
- [Dra00] T. G. Draper. Addition on a Quantum Computer. *arXiv e-print*, 2000.
- [GR02] L. Grover and T. Rudolph. Creating superpositions that correspond to efficiently integrable probability distributions. *arXiv preprint quant-ph/0208112*, 2002.

- [Gri94a] M. Griebel. Multilevel Algorithms Considered as Iterative Methods on Semidefinite Systems. *SIAM Journal on Scientific Computing*, 15(3):547–565, May 1994.
- [Gri94b] M. Griebel. *Multilevelmethoden Als Iterationsverfahren Über Erzeugendensystemen*. Teubner Skripten Zur Numerik. Vieweg+Teubner Verlag, Wiesbaden, 1994.
- [Gro98] L. K. Grover. Quantum Computers Can Search Rapidly by Using Almost Any Transformation. *Physical Review Letters*, 80(19):4329–4332, May 1998.
- [GSLW19] A. Gilyén, Y. Su, Guang H. Low, and N. Wiebe. Quantum singular value transformation and beyond: Exponential improvements for quantum matrix arithmetics. In *Proceedings of the 51st Annual ACM SIGACT Symposium on Theory of Computing*, pages 193–204, June 2019.
- [HHL09] A. W. Harrow, A. Hassidim, and S. Lloyd. Quantum algorithm for solving linear systems of equations. *Physical Review Letters*, 103(15):150502, October 2009.
- [Hip06] R. Hiptmair. Operator preconditioning. *Comput. Math. Appl.*, 52(5):699–706, 2006.
- [HJZ23] J. Hu, S. Jin, and L. Zhang. Quantum algorithms for multiscale partial differential equations. *arXiv preprint arXiv:2304.06902*, 2023.
- [HSS08] H. Harbrecht, R. Schneider, and C. Schwab. Multilevel frames for sparse tensor product spaces. *Numerische Mathematik*, 110(2):199–220, August 2008.
- [HW89] C. E. Heil and D. F. Walnut. Continuous and Discrete Wavelet Transforms. *SIAM Review*, 31(4):628–666, December 1989.
- [JLY23] S. Jin, N. Liu, and Y. Yu. Quantum simulation of partial differential equations: Applications and detailed analysis. *Phys. Rev. A*, 108:032603, Sep 2023.
- [Kit95] A. Y. Kitaev. Quantum measurements and the Abelian Stabilizer Problem. *arXiv e-prints*, 1995.
- [KM01] P. Kaye and M. Mosca. Quantum networks for generating arbitrary quantum states. In *International Conference on Quantum Information*, page PB28. Optica Publishing Group, 2001.
- [Lin22] L. Lin. Lecture notes on quantum algorithms for scientific computation. *arXiv preprint arXiv:2201.08309*, 2022.
- [LT20] L. Lin and Y. Tong. Optimal polynomial based quantum eigenstate filtering with application to solving quantum linear systems. *Quantum*, 4:361, November 2020.
- [Luo20] A. Luongo. Quantum algorithms for data analysis. <https://quantumalgorithms.org>, 2020.
- [MBA⁺23] S. A. Moses, C. H. Baldwin, M. S. Allman, R. Ancona, L. Ascarrunz, C. Barnes, J. Bartolotta, B. Bjork, P. Blanchard, M. Bohn, et al. A race-track trapped-ion quantum processor. *Physical Review X*, 13(4):041052, 2023.
- [Md23] N. S. Mande and R. de Wolf. Tight Bounds for Quantum Phase Estimation and Related Problems. *arXiv e-prints*, 2023.
- [MNUT24] S. Mohr, Y. Nakatsukasa, and C. Urzúa-Torres. Full operator preconditioning and the accuracy of solving linear systems. *IMA Journal of Numerical Analysis*, <https://doi.org/10.1093/imanum/drad104>, 2024.
- [MP16] A. Montanaro and S. Pallister. Quantum algorithms and the finite element method. *Physical Review A*, 93(3):032324, March 2016.
- [MP20] A. Målqvist and D. Peterseim. *Numerical homogenization by localized orthogonal decomposition*. SIAM, 2020.
- [MRTC21] J. M. Martyn, Z. M. Rossi, A. K. Tan, and I. L. Chuang. Grand unification of quantum algorithms. *PRX Quantum*, 2:040203, Dec 2021.
- [Nan20] G. Nannicini. An introduction to quantum computing, without the physics. *SIAM Review*, 62(4):936–981, 2020.
- [Osw90] P. Oswald. On Function Spaces Related to Finite Element Approximation Theory. *Zeitschrift für Analysis und ihre Anwendungen*, 9(1):43–64, February 1990.
- [Osw94] P. Oswald. *Multilevel Finite Element Approximation*. Teubner Skripten Zur Numerik. Vieweg+Teubner Verlag, Wiesbaden, 1994.
- [PS12] D. Peterseim and S. Sauter. Finite Elements for Elliptic Problems with Highly Varying , Nonperiodic Diffusion Matrix. *Multiscale Modeling & Simulation*, 10(3):665–695, January 2012.
- [Qis23] Qiskit contributors. Qiskit: An open-source framework for quantum computing, 2023.

- [Sch98] C. Schwab. *p- and hp-finite element methods*. Numerical Mathematics and Scientific Computation. The Clarendon Press, Oxford University Press, New York, 1998. Theory and applications in solid and fluid mechanics.
- [SSO19] Y. Subaşı, R. D. Somma, and D. Orsucci. Quantum Algorithms for Systems of Linear Equations Inspired by Adiabatic Quantum Computing. *Physical Review Letters*, 122(6):060504, February 2019.
- [SWR⁺23] Y. Sato, H. C. Watanabe, R. Raymond, R. Kondo, K. Wada, K. Endo, M. Sugawara, and N. Yamamoto. Variational quantum algorithm for generalized eigenvalue problems and its application to the finite-element method. *Physical Review A*, 108(2):022429, 2023.
- [SX18] C. Shao and H. Xiang. Quantum Circulant Preconditioner for Linear System of Equations. *Physical Review A*, 98(6):062321, December 2018.
- [TAWL21] Y. Tong, D. An, N. Wiebe, and L. Lin. Fast inversion, preconditioned quantum linear system solvers, and fast evaluation of matrix functions. *Physical Review A*, 104(3):032422, September 2021.
- [TLDE23] C. J. Trahan, M. Loveland, N. Davis, and E. Ellison. A variational quantum linear solver application to discrete finite-element methods. *Entropy*, 25(4):580, 2023.
- [Vid03] G. Vidal. Efficient Classical Simulation of Slightly Entangled Quantum Computations. *Physical Review Letters*, 91(14):147902, October 2003.
- [Xu92] J. Xu. Iterative methods by space decomposition and subspace correction. *SIAM Rev.*, 34(4):581–613, 1992.
- [Zal98] C. Zalka. Simulating quantum systems on a quantum computer. *Proceedings of the Royal Society of London. Series A: Mathematical, Physical and Engineering Sciences*, 454(1969):313–322, January 1998.

APPENDIX A. COMPRESSED ENCODING OF FINITE ELEMENT VECTORS

To solve a linear system on a quantum computer, we need to encode the right-hand side $|r\rangle$ and possibly the vector $|m\rangle$ for which we want to measure $m^T c$. We focus here on r , but the construction of m follows exactly the same techniques. The way r should be provided is as a quantum circuit U_r , which we require to map the zero state to $|r\rangle = |r\rangle_K$. Using the method independently discovered in [GR02, KM01, Zal98], such a circuit can be constructed from K quantum circuits $U_r^{(1)}, \dots, U_r^{(K)}$, which realize the functions

$$x \in \{0, 1\}^k \mapsto g_k(x) := \sum_{y \in \{0, 1\}^{K-k}} |r_{x \cdot y}|^2 \in \mathbb{R}$$

for $1 \leq k \leq K$. Here, the operation \cdot denotes concatenation of bit strings and $x \cdot y$ is to be understood as an integer index (indexing starts at zero). More precisely, $U_r^{(k)}$ implements the mapping

$$|x\rangle_{k-1} |0\rangle \mapsto |x\rangle_{k-1} \left(\sqrt{\frac{g_k(x \cdot 0)}{g_{k-1}(x)}} |0\rangle + \sqrt{\frac{g_k(x \cdot 1)}{g_{k-1}(x)}} |1\rangle \right).$$

The behavior of the mapping on the state $|x\rangle |1\rangle$ may be arbitrary. The same is true if the denominator $g_{k-1}(x)$ is zero. If some of the components of r are negative we also need an additional oracle U_r^\pm that flips the phase of the corresponding states. One can then easily check that

$$U_r := U_r^\pm \circ U_r^{(K)} \circ (I_1 \otimes U_r^{(K-1)}) \circ \dots \circ (I_{K-1} \otimes U_r^{(1)})$$

has the desired properties.

In the finite element context we usually want to construct a vector representation r of the bounded linear functional f^* acting on finite element functions. This functional is given by its Riesz representation f in the space L^2 and the components of r are computed as $r_j = (\Lambda_j^{(L)}, f)_{L^2}$. Here f is usually either provided as a symbolic formula, or constructed

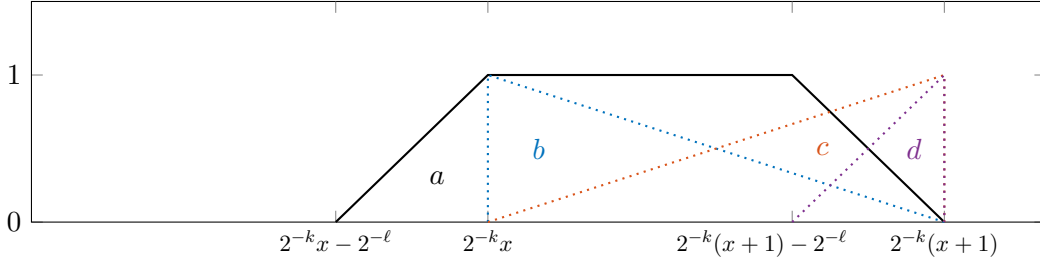


FIGURE A.1. Visualization of the function $\Lambda_{k,x}^{(\ell)}$ as the sum of 4 “half” basis functions $a + b + c - d$.

from some real word data such as measurements. Since the same is true for classical computers it is reasonable to assume that these inner products can be computed efficiently, and that the same is true for inner products with basis functions on coarser levels $(\Lambda_j^{(\ell)}, f)_{L^2}$ for $1 \leq \ell \leq L$ and $0 \leq j \leq (2^\ell - 1)^d$. This then implies that the values can also be computed efficiently on a quantum computer, but the computation must scale at least linearly with the amount of data contained in f . For a typical use case, this will not change the asymptotic runtime of the algorithm, since the amount of data is almost always constant and independent of the discretization parameters.

The computation of the described inner products is (almost) sufficient to efficiently compute even the preconditioned vector $|F^T r\rangle$. First, we describe the non-preconditioned case. There we see that g_k can be computed as

$$g_k(x) = \sum_{y \in \{0,1\}^{dL-k}} (\Lambda_{x,y}^{(L)}, f)_{L^2} = (\Lambda_{k,x}^{(L)}, f)_{L^2}.$$

where for $1 \leq \ell \leq L$, $1 \leq k \leq d\ell$, and $0 \leq x \leq (2^k - 1)^d$ we define

$$\Lambda_{k,x}^{(\ell)} := \sum_{y=2^{d\ell-k}x}^{2^{d\ell-k}(x+1)-1} \Lambda_y^{(\ell)}.$$

A visualization of this function can be seen in Figure A.1. It is unclear whether the inner products with these functions could be computed efficiently from the inner products with the basis functions, but one can see that each $\Lambda_{k,x}^{(\ell)}$ is a sum of “half” basis functions, and we present a visual proof in Figure A.1 in the one-dimensional case.

For the preconditioned case, the preparation of the states for the right hand side is more complicated due to the fact that we have to assemble the preconditioned state $|F^T r\rangle$ directly. For simplicity, let us assume that there are some $\tilde{L} \in \mathbb{N}$ such that $L = 2^{\tilde{L}}$. For the computation of g_k we then consider two cases separately. First, for $1 \leq k \leq \tilde{L}$ the variable x in each $g_k(x)$ refers only to the grid level ℓ on which information is acquired. Instead of giving an explicit formula for g_k , it is sufficient to understand that the combined transformation $O_r^{(\tilde{L})} \circ \dots \circ O_r^{(1)}$ is given by

$$|0\rangle_{\tilde{L}} \mapsto \frac{1}{\omega} \sum_{\ell=1}^L 2^{-\ell} (\Lambda_{\ell,0}^{(\ell)}, f)_{L^2} |\ell\rangle$$

where $\omega := (\sum_{\ell=1}^L 2^{-2\ell} (\Lambda_{\ell,0}^{(\ell)}, f)_{L^2}^2)^{-1/2}$ is a normalization factor. The total time to compute this is $\mathcal{O}(L)$, since it is a sum of L summands, each of which can be computed in $\mathcal{O}(1)$ time.

For $\tilde{L} + 1 \leq k \leq dL + \tilde{L}$ on the other hand we interpret x as consisting of the level ℓ and a spatial part z . The computation is almost the same as in the non-preconditioned case, differing only in the diagonal scaling of the preconditioner

$$g_k(\ell, z) = 2^{-\ell} (\Lambda_{k-\tilde{L},z}^{(\ell)}, f)_{L^2}$$

where the circuits will behave correctly if we artificially define $g_{\tilde{L}} \equiv 1$. Obviously, from the previous considerations, this can also be computed in time $\mathcal{O}(1)$, i.e. for the entire encoding procedure we obtain a runtime of $\mathcal{O}(L)$.

It has been shown that polynomials satisfy the requirements of this construction [MP16] and as such can be efficiently encoded. Similarly, one can check that the same is true for the basis functions $\Lambda_j^{(\ell)}$ and linear combinations thereof. However, a detailed analysis of the kind of functions that can be encoded does not exist to the best of our knowledge.

APPENDIX B. PROOF OF PROPOSITION 3.5

To prove the proposition, Figure B.1 gives quantum circuits that implement the block encodings for each operation with the exact normalization γ . Additionally, the bounds on the subnormalization $\tilde{\gamma}$ follows from lower bounds on the norm of the resulting matrix as follows.

- $A \otimes B$: An easy calculation shows that

$$\begin{aligned} \gamma_A \gamma_B (\Pi_{A,2} \otimes \Pi_{B,2}) (U_A \otimes U_B) (\Pi_{A,1} \otimes \Pi_{B,1})^\dagger \\ = (\gamma_A \Pi_{A,2} U_A \Pi_{A,1}^\dagger) \otimes (\gamma_B \Pi_{B,2} U_B \Pi_{B,1}^\dagger) = A \otimes B \end{aligned}$$

and we can exactly calculate the norm as $|A \otimes B| = |A| |B|$. For constructing the C_{Π} NOT operations we use that a state is in the range of a projection $\Pi_{A,\bullet} \otimes \Pi_{B,\bullet}$ exactly if it is in the range of $\Pi_{A,\bullet} \otimes \text{Id}$ and in the range of $\text{Id} \otimes \Pi_{B,\bullet}$. For computing the logical and of two boolean values in a quantum computer the Toffoli is used. The two original values need to be uncomputed subsequently.

- A^\dagger : An easy calculation shows that

$$\gamma_A \Pi_{A,1} U_A^\dagger \Pi_{A,2}^\dagger = (\gamma_A \Pi_{A,2} U_A \Pi_{A,1}^\dagger)^\dagger = A^\dagger$$

and we can exactly calculate the norm as $|A^\dagger| = |A|$.

- $\begin{bmatrix} A & 0 \\ 0 & B \end{bmatrix} =: D$: Let us first assume that the block encodings for both A and B have the same normalization $\gamma_A = \gamma_B$. Then we can calculate

$$\begin{aligned} \gamma_A (\Pi_{A,2} \otimes |0\rangle\langle 0| + \Pi_{B,2} \otimes |1\rangle\langle 1|) (U_A \otimes |0\rangle\langle 0| + U_B \otimes |1\rangle\langle 1|) \\ (\Pi_{A,1} \otimes |0\rangle\langle 0| + \Pi_{B,1} \otimes |1\rangle\langle 1|)^\dagger \\ = (\gamma_A \Pi_{A,2} U_A \Pi_{A,1}^\dagger) \otimes |0\rangle\langle 0| + (\gamma_B \Pi_{B,2} U_B \Pi_{B,1}^\dagger) \otimes |1\rangle\langle 1| = D \end{aligned}$$

If the encodings do not have the same normalization, then it is possible to increase the lower of the two normalizations, though this needs an additional qubit. For the matrix norm we know that $|D| = \max\{|A|, |B|\}$.

- AB : Indeed the construction works without the extra requirement on the size of the matrices, which instead is only needed to bound the subnormalization. The validity of the encoding follows from

$$\begin{aligned} & \gamma_A \gamma_B (\Pi_{A,2} \otimes \langle 1|) (U_A \otimes \text{Id}_2) C_{\Pi_{A,1}} \text{NOT}(U_B \otimes \text{Id}_2) (\Pi_{B,1} \otimes \langle 0|)^\dagger \\ &= \gamma_A \gamma_B \Pi_{A,2} U_A (\text{Id} \otimes \langle 1|) C_{\Pi_{A,1}} \text{NOT}(\text{Id} \otimes |0\rangle) U_B \Pi_{B,1}^\dagger \\ &= (\gamma_A \Pi_{A,2} U_A \Pi_{A,1}^\dagger) (\gamma_B \Pi_{B,2} U_B \Pi_{B,1}^\dagger) = AB \end{aligned}$$

where we used that by definition $(\text{Id} \otimes \langle 1|) C_{\Pi_{A,1}} \text{NOT}(\text{Id} \otimes |0\rangle) = \Pi_{A,1}^\dagger \Pi_{A,1}$. The projections $\Pi_\bullet \otimes \langle 0|$ can be constructed similar to the ones in the $A \otimes B$ case. Finally we need a lower bound on the matrix norm of the product. For this consider

$$|A| |B| \leq |AB| |B^+| |B| = \kappa(B) |AB|$$

where we have to assume that $m_B \geq n_B$ and equivalently we get $\kappa(A) |AB| \geq |A| |B|$ if $n_A \geq m_A$. The bounds for the subnormalization follow by straightforward calculation.

- $\begin{bmatrix} A & B \end{bmatrix}$: This matrix can be constructed from (4) using the equality

$$\begin{bmatrix} A & B \end{bmatrix} = (\begin{bmatrix} \gamma_A & \gamma_B \end{bmatrix} \otimes \text{Id}) \begin{bmatrix} A/\gamma_A & 0 \\ 0 & B/\gamma_B \end{bmatrix}$$

where $\begin{bmatrix} \gamma_A & \gamma_B \end{bmatrix}$ is encoded by a Y -rotation with normalization $\sqrt{\gamma_A^2 + \gamma_B^2}$ and the block square matrix due to the scaling has normalization 1. The subnormalization can be calculated using

$$\left| \begin{bmatrix} A & B \end{bmatrix} \right| \leq \sqrt{|A|^2 + |B|^2}$$

- $\mu_A A + \mu_B B$: This can similarly be constructed from (4) by

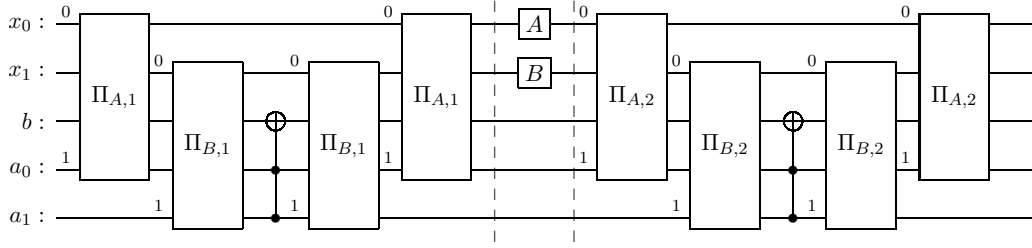
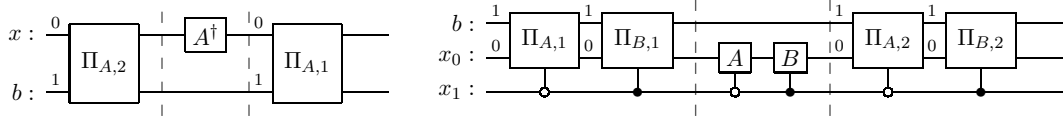
$$\mu_A A + \mu_B B = (\begin{bmatrix} \sqrt{\gamma_A \mu_A} & \sqrt{\gamma_B \mu_B} \end{bmatrix} \otimes \text{Id}) \begin{bmatrix} A/\gamma_A & 0 \\ 0 & B/\gamma_B \end{bmatrix} \left(\begin{bmatrix} \sqrt{\gamma_A \mu_A} \\ \sqrt{\gamma_B \mu_B} \end{bmatrix} \otimes \text{Id} \right)$$

where the left and right vectors lead to a total subnormalization of $\gamma_A \mu_A + \gamma_B \mu_B$. As mentioned the matrix norm of a sum can in general not be bounded from below.

[†] INSTITUTE OF MATHEMATICS, UNIVERSITY OF AUGSBURG, UNIVERSITÄTSSTR. 12A, 86159 AUGSBURG, GERMANY

^{*} CENTRE FOR ADVANCED ANALYTICS AND PREDICTIVE SCIENCES (CAAPS), UNIVERSITY OF AUGSBURG, UNIVERSITÄTSSTR. 12A, 86159 AUGSBURG, GERMANY

Email address: {matthias.deiml,daniel.peterseim}@uni-a.de


 (a) Block encoding for $A \otimes B$

 (b) Block encoding for A^\dagger

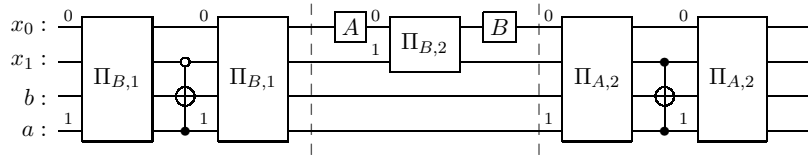
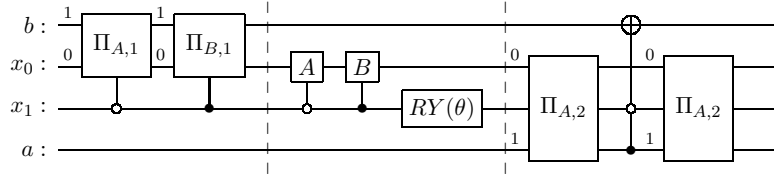
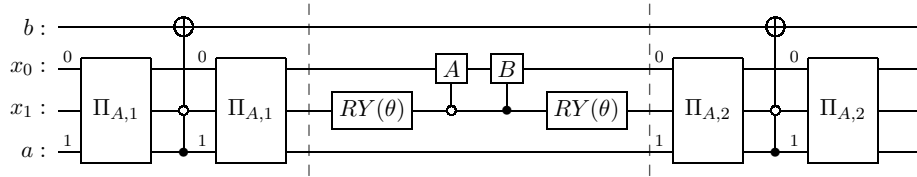
 (c) Block encoding for $\begin{bmatrix} A & 0 \\ 0 & B \end{bmatrix}$

 (d) Block encoding for AB

 (e) Block encoding for $\begin{bmatrix} A & B \end{bmatrix}$ where $\theta = \arctan(\gamma_B/\gamma_A)$

 (f) Block encoding for $\mu_A A + \mu_B B$ where $\theta = \arctan(\sqrt{\gamma_B \mu_B / (\gamma_A \mu_A)})$

FIGURE B.1. Block encodings for the operations of Proposition 3.5.